

JAERI-Research
99-071



JP0050132



**EXPERIMENTAL STUDY ON THE INFLUENCE OF RADIATION
ON HIGH-VOLTAGE INSULATION GASES**

December 1999

**Yukio FUJIWARA, Takashi INOUE, Kenji MIYAMOTO, Naoki MIYAMOTO,
Yoshihiro OHARA, Yoshikazu OKUMURA and Kazuhiro WATANABE**

日本原子力研究所
Japan Atomic Energy Research Institute

本レポートは、日本原子力研究所が不定期に公刊している研究報告書です。
入手の間合わせは、日本原子力研究所研究情報部研究情報課（〒319-1195 茨城県那珂郡東海村）あて、お申し越しください。なお、このほかに財団法人原子力弘済会資料センター（〒319-1195 茨城県那珂郡東海村日本原子力研究所内）で複写による実費領布をおこなっております。

This report is issued irregularly.

Inquiries about availability of the reports should be addressed to Research Information Division, Department of Intellectual Resources, Japan Atomic Energy Research Institute, Tokai-mura, Naka-gun, Ibaraki-ken, 319-1195, Japan.

© Japan Atomic Energy Research Institute, 1999

編集兼発行 日本原子力研究所

Experimental Study on the Influence of Radiation on High-voltage Insulation Gases

Yukio FUJIWARA, Takashi INOUE, Kenji MIYAMOTO, Naoki MIYAMOTO ,
Yoshihiro OHARA, Yoshikazu OKUMURA and Kazuhiro WATANABE

Department of Fusion Engineering Research
Naka Fusion Research Establishment
Japan Atomic Energy Research Institute
Naka-machi, Naka-gun, Ibaraki-ken

(Received November 29,1999)

In a neutral beam injection (NBI) system for next generation tokamaks such as International Thermonuclear Experimental Reactor (ITER), insulation gas around a beam source will be irradiated with neutrons and gamma rays from the reactor. It is necessary to evaluate the influence of the radiation on the insulation gas for the engineering design of the ITER-NBI system. In the present paper, the influence of the ^{60}Co gamma rays on air, SF_6 , C_2F_6 , CO_2 , and mixing gas of air and SF_6 was studied. Ionization current and voltage-holding characteristics of the gases were measured for an absorbed dose rate of 0.45 Gy/s using parallel disk electrodes whose diameter is 130 mm. Saturation current proved to increase linearly with a gap length between the electrodes, gas pressure, an absorbed dose rate, and molecular weight of the gases. Voltage-holding capability was degraded by about 10 %; the degree of the degradation did not depend on the absorbed dose rate. Dissociative products of SF_6 by the irradiation were also analyzed with a quadrupole mass spectrometer. New peaks that did not exist before irradiation appeared at the m/e of 48, 64, 67, 83, 86, 102, and 105 after irradiation. The amount of the dissociative products turned out to be saturated at a higher absorbed dose.

Keywords: ITER, NBI, Radiation Induced Conductivity, Gas Insulation, Insulation Gas, Gamma Rays, Ionization Current, Breakdown, SF_6 , Dissociative Product

高電圧用絶縁ガスに及ぼす放射線の影響に関する実験的研究

日本原子力研究所那珂研究所核融合工学部

藤原 幸雄・井上多加志⁺・宮本 賢治・宮本 直樹・小原 祥裕・奥村 義和・渡辺 和弘

(1999 年 11 月 29 日 受理)

国際熱核融合実験炉(ITER)をはじめとする次世代のトカマク型核融合炉において、中性粒子入射装置(NBI)のビーム源まわりの絶縁に使用される絶縁ガスは、炉からの中性子やガンマ線などの放射線にさらされる。したがって、ITER-NBI の工学設計を行うにあたり、絶縁ガスに対する放射線の影響を評価しておくことが必要となる。本論文は、空気・SF₆・C₂F₆・CO₂ならびに空気と SF₆ の混合ガスに対する ⁶⁰Co ガンマ線の影響を調べたものである。各種ガスの電離電流および耐電圧特性が直径130mmの円盤状平行電極を用いて吸収線量率0.45Gy/sの条件で調べられた。飽和電流は電極間のギャップ長、ガス圧、吸収線量率、ならびにガスの分子量に比例することが明らかとなった。耐電圧性能は、ガンマ線照射により 10%程度低下するものの、その程度は吸収線量率に依存しなかった。また、質量分析器を用いて、ガンマ線照射による SF₆ ガスの分解生成物も調べられた。照射後、未照射の場合には存在しなかったピークが m/e = 48、64、67、83、86、102、105 のところに確認された。SF₆ ガスの分解生成物量は吸収線量が高くなるにつれて飽和することがわかった。

CONTENTS

1. Introduction	1
2. Experimental Apparatus	2
2.1 Apparatus for Measuring Ionization Current and Voltage-holding Characteristics	2
2.2 Apparatus for Measuring Dissociation of SF ₆ Gas	3
3. Experimental Result	3
3.1 Applied Voltage Dependence	3
3.2 Gap Length Dependence	5
3.3 Pressure Dependence of SF ₆ Gas	5
3.4 Absorbed Dose Rate Dependence of SF ₆ Gas	5
3.5 Dissociation of SF ₆ Gas	6
4. Discussion	6
4.1 Ionization Current Characteristics	6
4.2 Estimation of Ionization Current at the ITER-NBI System	7
4.3 Influence of Radiation Species and Their Energy on Ionization Current	8
4.4 Dissociation of SF ₆ Gas	9
5. Summary	10
Acknowledgments	10
References	11

目 次

1. はじめに	1
2. 実験装置	2
2.1 電離電流と耐電圧特性を調べる装置	2
2.2 SF ₆ ガスの分解を調べる装置	3
3. 実験結果	3
3.1 電圧特性	3
3.2 ギャップ長依存性	5
3.3 SF ₆ ガスの場合の圧力依存性	5
3.4 SF ₆ ガスの場合の吸収線量率依存性	5
3.5 SF ₆ ガスの分解	6
4. 考察	6
4.1 電離電流特性	6
4.2 ITER-NBI システムにおける電離電流の評価	7
4.3 電離電流に対する放射線の種類とエネルギーの影響	8
4.4 SF ₆ ガスの分解	9
5. まとめ	10
謝 辞	10
参考文献	11

1. Introduction

In nuclear fusion research, neutral beam injection (NBI) has been the most successful scheme to heat magnetically confined plasmas.⁽¹⁾⁽²⁾ It is also a promising candidate to drive plasma current as well as to heat a plasma in next generation tokamaks such as International Thermonuclear Experimental Reactor (ITER). Figure 1.1 shows a plan view of the ITER-NBI system, which is designed to deliver 50 MW of 1 MeV D^0 beams into the plasma with three injector modules.⁽³⁾ Figure 1.2 shows an isometric view of the three injector modules. Figure 1.3 shows cross sectional view of one injector module. Each module is equipped with a beam source, which generates 1 MeV D^+ beams of 40 A for a duration longer than 1000 sec.⁽⁴⁾⁽⁵⁾

The D^+ beams of 1 MeV are produced using an electrostatic accelerator whose electrical potential is 1 MV. Thus, the beam source has to be insulated electrically from a beam-source vessel that is at ground potential. In the engineering design of the ITER-NBI system, insulation gas is utilized for 1-MV insulation between the beam source and the beam-source vessel. The insulation gas is irradiated with radiation such as neutrons, X-rays, and gamma rays from the reactor. Subsequently, the insulation gas will be ionized and dissociated. Ionization current flowing through the insulation gas will result in loss of electric power and increase of gas temperature. Dissociation of the gas might cause voltage-holding degradation. Furthermore, dissociative products from the gas might be harmful to human body.

E. Hodgson has studied ionization current of Helium, N_2 , air, CO_2 , and SF_6 at atmospheric pressure with an experimental setup of about 3 cc using electron beams.⁽⁶⁾ On the basis of his experimental results, he extrapolated ionization current at the ITER-NBI conditions. According to his extrapolation, ionization current would be so high that a large amount of acceleration power of several MW would dissipate inside the vessel. However, it is not clear that his extrapolation is applicable to the ITER-NBI system, since there is much difference between his experimental condition and the ITER-NBI condition in volume and gas pressure. In the ITER-NBI system, gas volume is about 30 m^3 , and gas pressure is several bar. For this reason, it has become a very important issue to obtain database on ionization current of insulation gas for the engineering design of the ITER-NBI system.

As for dissociation of insulation gas, H. Yoshida et al. have measured dissociative products of SF_6 using the ^{60}Co gamma rays.⁽⁷⁾ They demonstrated that poisonous gas of S_2F_{10} does not be produced by the gamma rays. However, experimental results they obtained were influenced by impurities on the surface of gas ampules, so that relationship between absorbed dose and quantity of dissociative products has not been clear.

To clarify the influence of radiation more quantitatively, we performed an irradiation experiment using the ^{60}Co gamma rays. With parallel disk electrodes of 130 mm in diameter, we studied ionization current and voltage-holding characteristics of air, CO_2 , C_2F_6 , SF_6 , SF_6 mixed with air, while changing gap length between the electrodes, gas pressure, and dose rate. Further, we studied dissociation of SF_6 with a quadrupole mass spectrometer measuring mass spectra up to $m/e = 200$. To reduce the influence of impurities, we degreased and baked gas containers before gas introduction. In the present paper, after a description of experimental apparatus, experimental results on ionization current, voltage-holding characteristics, and dissociation of SF_6 are described in order. Then an experimental formula is presented to estimate saturation current of insulation gases.

2. Experimental apparatus

2.1 Apparatus for measuring ionization current and voltage-holding characteristics

Insulation gases were irradiated with the ^{60}Co gamma rays in an irradiation facility at JAERI-Tokai. The facility has two kinds of gamma-ray sources. Radioactivity of the sources is 4.1×10^{15} Bq, and 0.22×10^{15} Bq, respectively. The sources are 134 mm in outer diameter and 405 mm in height. Relations between absorbed dose rate and distance from the sources are shown in Fig. 2.1. The absorbed dose rate was defined as that for air: the absorbed dose rate in Gy/s was calculated by multiplying exposure in C/kg/s by the average energy needed to produce a pair of electron and positive ion (W-value) of air in eV, which is 33.8 eV for the ^{60}Co gamma rays.

Figure 2.2 shows experimental apparatus for measuring ionization current and breakdown voltage. The apparatus is composed of a test chamber, electrical cables, and a power supply. The test chamber consists of a circular pyrex-glass, upper and lower flanges, a bourdon-tube pressure gauge, a linear motion introducer, a gas supply line, and parallel disk electrodes made of stainless steel. The pyrex-glass has an internal diameter of 161 mm, an external diameter of 180 mm, and a height of 204 mm. The volume of the test chamber is about 4 liter. The bourdon-tube pressure gauge shows the pressure of test gas filled in the chamber. The linear motion introducer enables us to change the gap length between the parallel disk electrodes at the range of 0 mm to 20 mm. After the test chamber is evacuated, test gas is introduced through the gas line. The disk electrodes are 130 mm in diameter and 5 mm in thickness. The cathode electrode is insulated by a 8-mm thick teflon disk. Further, an electrical cable connected to the cathode electrode is insulated with a ceramic break to distinguish ionization current generated between the electrodes from that generated at other

space. Capacity of the power supply is DC 100 kV, 3 mA.

The gamma rays ionize test gas by interactions of the photoelectric effect, the Compton effect, and the pair production of electron and positron, as shown in Fig. 2.3. Produced charged particles are attracted toward the electrodes by an electric field. Ionization current is measured as voltage drop in a resistor of 10 k ohm.

2.2 Apparatus for measuring dissociation of SF₆ gas

Figure 2.4 illustrates experimental apparatus for analyzing dissociative products from SF₆ gas. The apparatus consists of gas lines, a vacuum tank, vacuum pumps, a quadrupole mass spectrometer, and a pen recorder. The quadrupole mass spectrometer is capable of measuring mass spectra up to $m/e = 200$. Figure 2.5 shows a gas container whose volume is about 0.03 liter. The container made of stainless steel has been degreased. Thickness of the container is 1.5 mm; the attenuation of the gamma rays penetrating the container wall is negligible. The gas line is equipped with a needle valve regulating gas diffusion from the gas container to the vacuum tank. The vacuum tank is evacuated with an oil-sealed vacuum pump and a turbo-molecular pump.

Two gas containers were baked at over 150 °C for over 10 min during evacuation. After they were cooled down to room temperature, SF₆ gas was introduced into them. Then, one gas container was detached and then irradiated with the gamma rays. The other gas container was not irradiated for reference. The irradiated gas container was installed again to measure positive ion mass spectra. The volume of the gas flowing into the vacuum tank was regulated with the needle valve to keep the pressure of the tank at 7.0×10^{-6} Torr during mass analysis.

3. Experimental result

3.1 Applied voltage dependence

Ionization currents of air, SF₆, C₂F₆, CO₂, and mixing gas of air and SF₆ were measured for an absorbed dose rate of 0.45 Gy/s. Figure 3.1 shows ionization currents of the gases against applied voltage between the electrodes. Gas pressure was 600 mb. Ionization current of SF₆ was highest and that of air was lowest, while breakdown voltage of SF₆ was highest and that of air was lowest. Thus, SF₆ is the worst gas from the viewpoint of suppressing ionization current, although SF₆ is the best gas from the viewpoint of suppressing breakdown.

Characteristics of the ionization current are similar to those at conventional

ionization chambers. The curve of ionization current is composed of three parts, region I to region III. Region I is recombination region. Applied voltage, namely, electric field is low, so that both positive ions and electrons move at the low speed. Since charged particles at the low speed are easy to recombine, they are difficult to reach electrodes; ionization current is low. By increasing applied voltage, the speed of charged particles increase; the ratio of recombination decreases. Thus, ionization current increases with applied voltage. Region II is saturation or plateau region. The ionization current is saturated. In this region, the number of charged particles collected by the electrodes is almost equal to the number of ions produced by radiation. Region III is secondary ionization region. With higher voltage, the speed of electrons becomes so high that they cause secondary ionization, followed by electron avalanche and then breakdown.

Breakdown voltage and ionization current of SF_6 mixed with air are shown in Fig. 3.2. Vertical axis on the left is breakdown voltage, and that on the right is " I_{ION} ". For convenience, the new term of I_{ION} was defined as the ionization current at a half voltage of breakdown voltage; it is regarded as saturation current. The figure indicates that a small quantity of SF_6 raised breakdown voltage significantly, while I_{ION} was proportional to volume rate of SF_6 gas. For example, 5%- SF_6 mixture improved breakdown voltage by 32 %, while I_{ION} increased just by 21 %; a little SF_6 mixed with air proved to have lower ionization current and higher voltage-holding capability. This experimental result suggests that mixing gas will be effective from the viewpoint of suppressing ionization current with keeping voltage-holding capability.

Figure 3.3 shows I_{ION} versus molecular weight. Circle shows I_{ION} at the gap length of 16.1 mm. Triangle shows I_{ION} at the gap length of 8.1 mm. Molecular weight of mixing gases was defined as average molecular weight that is the sum of molecular weight multiplied by ratio of partial pressure. The figure shows that I_{ION} was proportional to molecular weight.

Table 3.1 is a summary of average relative dielectric strength of the gases. It is

Table 3.1 Averaged relative dielectric strength: each dielectric strength was normalized by that of SF_6

Gas Species	Relative Dielectric Strength
SF_6	1
C_2F_6	0.81
Air(80%) + SF_6 (20%)	0.75
Air(90) + SF_6 (10%)	0.69
Air(95%) + SF_6 (5%)	0.63
CO_2	0.51
Air	0.49

normalized by the dielectric strength of SF_6 gas.

3.2 Gap length dependence

Figure 3.4 shows I_{ION} as a function of the gap length between the electrodes. I_{ION} increased linearly with the gap length. Linear relationship between I_{ION} and the gap length indicates that there will be linear relationship between I_{ION} and the volume of gas.

When we extrapolate using the linear curve, I_{ION} is not zero at the gap length of 0 mm. We think that it may be attributed to the influence of a space between the electrodes and the pyrex glass; charged particles generated in the space can be collected by the electrodes. Further, it could be due to electrons emitted from the electrode surface by photoelectric effect.

Breakdown voltage of the gases is plotted as a function of the gap length in Fig. 3.5. Breakdown voltage increased with the gap length to the 0.73.

3.3 Pressure dependence of SF_6 gas

Ionization current of SF_6 gas was measured at different gas pressure. Figure 3.6 shows the ionization current of SF_6 against applied voltage. Gas pressures were 0.59 (600 mb), 0.1, 0.15 and 0.2 MPa. At a pressure of 0.59 MPa (600 mb), the gap length was not 4.0 mm but 4.1 mm. Figure 3.7 shows the pressure dependence of I_{ION} . As is shown in the figure, I_{ION} increased linearly with gas pressure.

Breakdown voltage of SF_6 is shown as a function of gas pressure in Fig. 3.8. Open signs are breakdown voltage without irradiation, and closed signs are that during irradiation. At both conditions, breakdown voltage increased with gas pressure to the 0.72; significant irradiation influence on breakdown voltage was not observed.

3.4 Absorbed dose rate dependence of SF_6 gas

Changing the distance from the gamma-ray source to the electrodes is equivalent to changing absorbed dose rate. Then, we measured ionization current and voltage-holding characteristics at different distance conditions. Figure 3.9 shows the linear relationship between I_{ION} and absorbed dose rate.

Breakdown voltage as a function of absorbed dose rate is shown in Fig. 3.10. As compared with breakdown voltage without irradiation, the degradation in breakdown voltage during irradiation was about 10 %. The figure also indicates that there was not clear relationship between the degradation of breakdown voltage and absorbed dose rate.

3.5 Dissociation of SF₆ gas

Figure 3.11 shows an example of mass spectra of SF₆ gas. Upper side of the figure is a part of a mass spectrum without irradiation. Lower side is a part of that after irradiation. As compared with the spectrum without irradiation, there were some different peaks at m/e of 102 and 105 in the spectrum after irradiation. We think that the peaks would be due to products generated by dissociation of SF₆ molecules.

Figure 3.12 shows a mass spectrum from m/e = 0 to 200 without irradiation and that after irradiation of 4.0×10^6 Gy. There were clear differences at the m/e of 67, 83, 86 and 105. The largest difference was at the m/e of 105. The ratio of the height of the peak at the m/e of 105 to that at the m/e of 127 (SF₅⁺) is plotted as a logarithmic function of absorbed dose in Fig. 3.13. This figure indicates that the amount of the dissociative product did not increase linearly but be saturated with absorbed dose.

4. Discussion

4.1 Ionization current characteristics

Before the experiment, we expected lower ionization current for SF₆ gas, because it is well known that SF₆ molecules are prone to attach electrons. However, experimental results showed that ionization current of SF₆ was highest. We think that this would be attributable to the electron-energy dependence of the electron-attachment cross section of a SF₆ molecule. Although the electron-attachment cross section at the energy of about 0 eV is very large, it is small at higher energy region.⁽⁸⁾ The energy of electrons generated by the interactions with the gamma rays is high, so that the electrons can not be attached to SF₆ molecules. Thus, the electrons can migrate in the gas, ionizing gas molecules successively.

On the basis of above experimental results, we derive an experimental formula for estimating saturation current. Saturation current, I_{sat} , generated by the ⁶⁰Co gamma rays is

$$I_{\text{sat}} [\text{A}] = f_{\text{gas}} \times M \times V \times P \times D \quad (4-1)$$

Here, f_{gas} is constant obtained from the present experiment, which was 0.00143.

M : molecular weight.

V : volume of gas (m³).

P : pressure of gas (atm).

D : absorbed dose rate at the case of air (Gy/s).

It should be noted that electric field between electrodes is assumed to be high enough to collect all charged particles generated by the gamma rays.

The observation of the linear relationship between saturation current and molecular weight is of interest. At the energy of the ^{60}Co gamma rays, a dominant interaction is Compton scattering. The cross section of Compton scattering increases proportionally with atomic number.⁽⁹⁾ Saturation current would, therefore, be proportional to the molecular weight at same gas pressure, same temperature and same volume.

4.2 Estimation of ionization current at the ITER-NBI system

Using the experimental formula, we estimated ionization current of insulation gases at the case of the ITER-NBI system. Figure 4.1 shows the cross section of the ITER-NBI module. The volume of the space between the beam source and the beam-source vessel is about 30 m^3 . Table 4.1 shows required gas pressure for each insulation gas around the beam source at the ITER-NBI system. At each pressure, dielectric capability of each gas is as same as that of CO_2 at 20 atm. According to the neutronics calculation, absorbed dose rate of air around the beam source will be about 0.1 Gy/s during operation of ITER.⁽¹⁰⁾ Then, we assumed an absorbed dose rate of 0.1 Gy/s, estimating total ionization current of each insulation gas. Table 4.2 is a summary of the ionization current. At the case of SF_6 , total ionization current was estimated to be 4.6 A. At the case of 5%- SF_6 and 95%-air mixing gas, total ionization current was estimated to be 2.1 A. Thus, power of several MW will be dissipated between the beam source and the beam-source vessel. From the viewpoint of capacity of electric power supply and cooling system, the ionization currents would not be acceptable. Other insulating method like vacuum insulation would be

Table 4.1 Required gas pressure for the ITER-NBI system: dielectric capability of each gas is as same as that of CO_2 at 20 atm.

Gas Species	Pressure [atm]
SF_6	7.9
C_2F_6	10.6
Air(80%) + SF_6 (20%)	11.8
Air(90%) + SF_6 (10%)	13.2
Air(95%) + SF_6 (5%)	15
Air	21.2
CO_2	20

Table 4.2 Total ionization current inside the beam-source vessel: ionization current was estimated from the experimental formula. Absorbed dose rate was assumed to be 0.1 Gy/s.

Gas Species	Current [A]
SF ₆	4.6
C ₂ F ₆	6.1
Air(80%) + SF ₆ (20%)	2.9
Air(90%) + SF ₆ (10%)	2.4
Air(95%) + SF ₆ (5%)	2.1
Air	2.6
CO ₂	3.9

necessary instead of gas insulation.

4.3 Influence of radiation species and their energy on ionization current

In general, cross sections of nuclear reactions are dependent on both radiation species and their energy. Thus, when using the above experimental formula, we must pay much attention to radiation species and their energy. It should be noted that the experimental formula is applicable at the case of the gamma rays whose dominant interaction is compton scattering.

By generalizing the experimental formula, we propose a formula that is applicable to all kinds of radiation. We think that saturation current of a gas will generally be proportional to volume of the gas, pressure of the gas, and absorbed dose rate of the gas, which is not absorbed dose rate of air. Then, we present a general formula of saturation current, $I_{\text{sat-general}}$, which is applicable to all kinds of radiation.

$$I_{\text{sat-general}} [\text{A}] = F_{\text{gas}} \times V \times P \times D_{\text{gas}} \quad (4-2)$$

Here, F_{gas} is dependent on gas species, radiation species, and energy spectrum.

V : volume of the gas (m³).

P : pressure of the gas (atm).

D_{gas} : absorbed dose rate of the gas (Gy/s).

Absorbed dose rate of the gas, D_{gas} , will depend on gas species, radiation species, and their energy spectrum. Even if same radiation is irradiated, the absorbed dose of a gas

Table 4.3 Relative intensity and presumed species appearing after irradiation of 4.0×10^6 Gy: the intensity at the m/e of 127 (SF_5^+) was defined as 1000. The absorbed dose of 4.0×10^6 Gy is equivalent to the absorbed dose of over forty-year operation of ITER

m/e	Relative Intensity	Presumed Species
105	5.2	SOF_3^+
102	0.8	S_2F_2^+ or SO_2F_2^+
86	1.6	SOF_2^+
83	1.4	S_2F^+ or SO_2F^+
67	2.6	SOF^+
64	0.4	SO_2^+ , S_2^+ ,
48	1	SO^+
127	1000	SF_5^+

will be different from that of other gas. This is why cross section of a gas species is different from that of other gas species. Furthermore, absorbed dose rate of a gas will change with energy spectrum of radiation, since cross section of nuclear reaction is dependent on radiation energy.

Insulation gas utilized at the ITER-NBI system will be subjected by not only gamma rays whose dominant interaction is compton scattering, but also neutrons and gamma rays which have broad range of energy spectrum. Thus, to evaluate ionization current of insulation gases more accurately, irradiation experiments with neutrons and gamma rays, which is the same energy spectrum at ITER, are desirable. In the irradiation experiments, small volume, low pressure, and low absorbed dose rate are enough as experimental conditions, since saturation current increases linearly with volume, pressure, and absorbed dose rate as demonstrated by the present experiment. If the factor of F_{gas} is evaluated by an experiment, total ionization current at the case of ITER-NBI system will be estimated using equation 4-2.

4.4 Dissociation of SF_6 gas

Table 4.3 shows relative intensity and presumed species appearing after irradiation. We think that the trend on the figure 3.13 will be similar to the absorbed dose dependence of the amount of dissociative products of SF_6 . If absorbed dose rate during operation of ITER is about 0.1 Gy/s, the absorbed dose of 4.0×10^6 Gy is higher than that for forty-year operation of ITER. From these results, the ratio of dissociative products by the gamma rays will be less than about 1.3 %, even though SF_6 is exposed for forty years at ITER.

5. Summary

The influence of radiation on insulation gases was studied with the ^{60}Co gamma rays. Using parallel disk electrodes, we investigated ionization currents and voltage-holding characteristics of air, SF_6 , C_2F_6 , CO_2 , and mixing gas of air and SF_6 . Saturation current proved to increase linearly with gap length between electrodes, gas pressure, absorbed dose rate, and molecular weight of gas. An experimental formula estimating saturation current was obtained on the basis of experimental results. A small quantity of SF_6 mixed with air proved to have lower ionization current and higher voltage-holding capability; mixture of SF_6 gas will be effective from the viewpoint of suppressing ionization current. Degradation of voltage-holding capability during irradiation proved to be about 10 %. The degree of the degradation did not depend on absorbed dose rate. Using the experimental formula, ionization current at the ITER-NBI system was estimated. The ionization current of all gases was so high that it would not be acceptable. Instead of gas insulation, other method like vacuum insulation would be necessary.

We also analyzed dissociative products from SF_6 by gamma-ray irradiation. Positive ion mass spectra after irradiation were compared with those without irradiation. New peaks that did not exist before irradiation appeared at the m/e of 48, 64, 67, 83, 86, 102, and 105. The amount of dissociative products proved to be saturated with absorbed dose. For an absorbed dose of 4×10^6 Gy, corresponding to over forty-year operation of ITER, the ratio of dissociative products of SF_6 was estimated to be about 1.3 %. Thus, the amount of dissociative products from SF_6 gas by gamma rays will be small.

Acknowledgments

We would like to acknowledge Mr. Nagayama for technical support at the ^{60}Co -gamma-rays irradiation facility. We would like to express our gratitude to Dr E. Hodgson for valuable information. We would like to thank Dr. P. L. Mondino, Dr. R. Hemsworth, and Dr. E. Di Pietro for their encouragement and valuable information. We would like to express our thanks to Dr. M. Ohta and Dr. S. Matsuda for their support and encouragement. We are grateful to other members of NBI heating laboratory for their valuable discussions and comments.

References

- [1] JT-60 Team presented by M.Kikuchi: 15th Int. Conf. on Plasma Physics and Controlled Nuclear Fusion Research, Sevilla, Spain (1994) A-1-I-2
- [2] K. M McGrire, et al.: The Physics of Plasma, Special Issue (1995)
- [3] ITER EDA Final Design Report, DDD 5.3, NB H&CD system
- [4] R. Hemsworth et al.: Proc. 16th IAEA Fusion Energy Conference, 927 (1996)
- [5] R. Hemsworth et al: Rev. Sci. Instrum. 67 (3), 1120 (1996)
- [6] E.Hodgson : Insulation gas Characterization, The 1st technical meeting, Cadarache 2-5 July 1996
- [7] H. Yoshida et al : JAERI-memo 04-122 (1992) (in Japanese)
- [8] M. Hayashi and T.Nimura : J. Phys., D17, 2215 (1984)
- [9] N.Tsoufanidis : Measurement and Detection of Radiation, Hemisphere Publication Corporation (1983)
- [10] T.Inoue et al.: Pro. 20th SOFT, Marseille, France, 7-11 September 1998

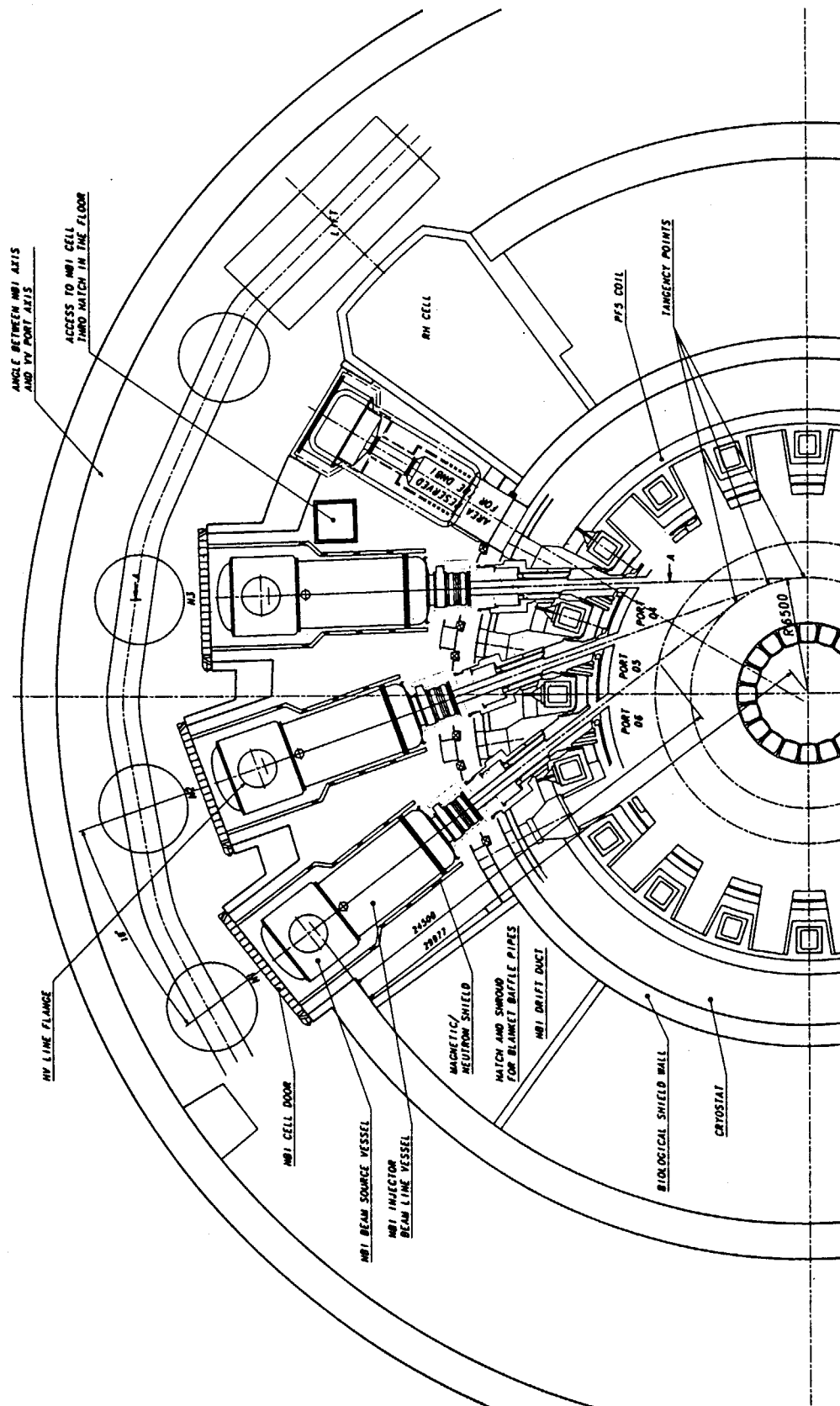


Figure 1.1 A plan view of the ITER-NBI system.

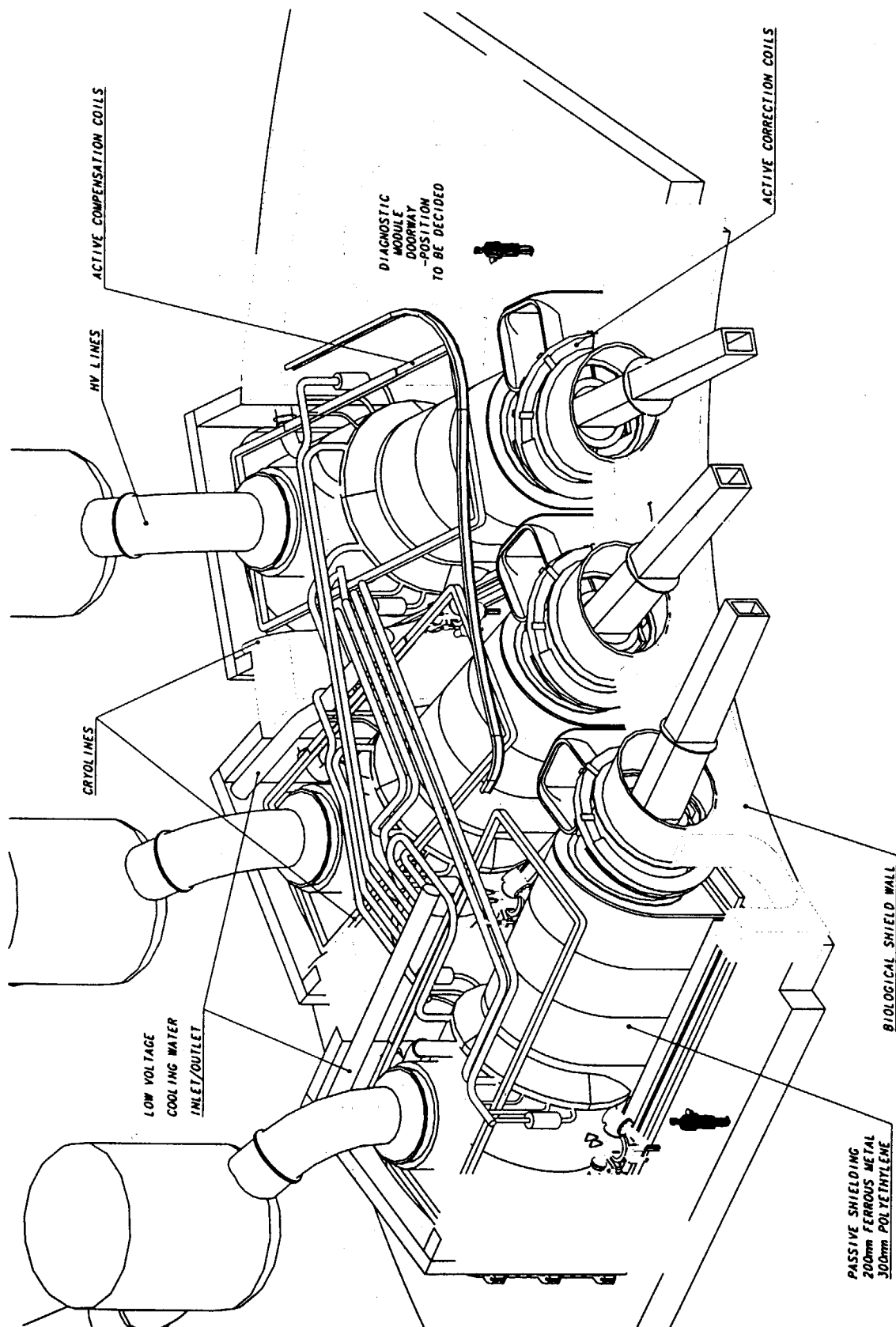


Figure 1.2 An isometric view of the three injector modules.

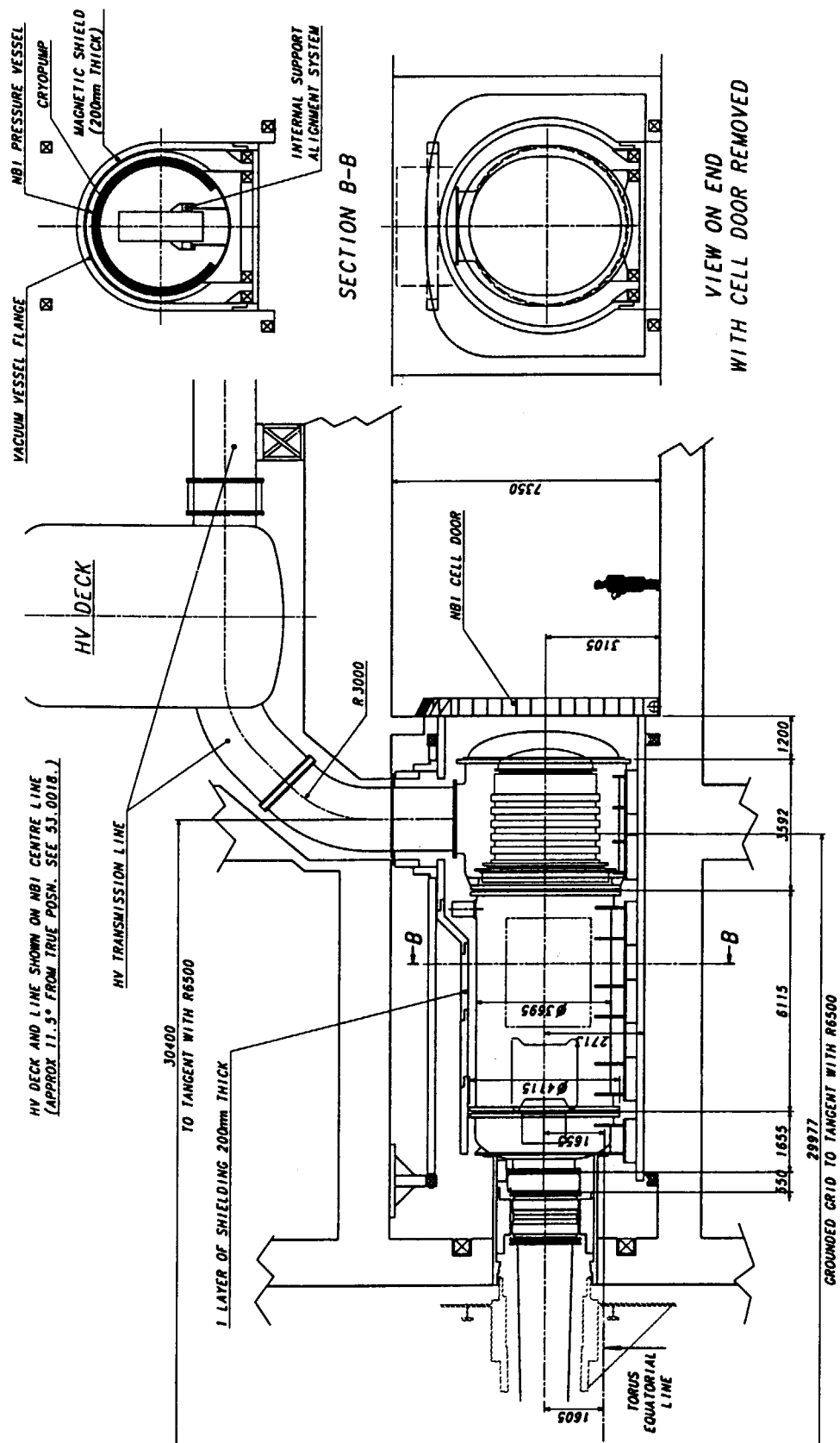
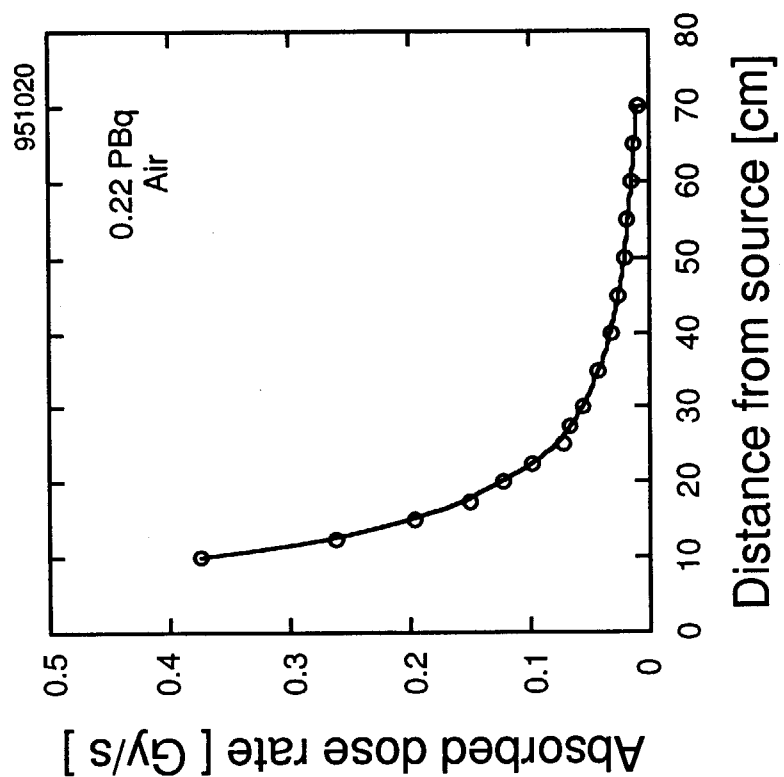
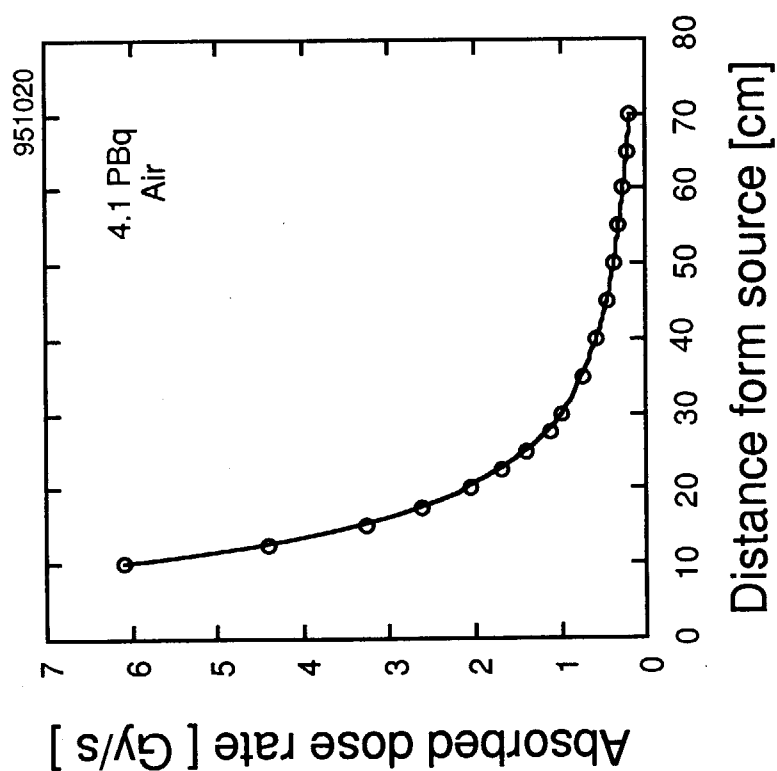


Figure 1.3 Cross section of the neutral beam injector module.



Gamma-ray source of 0.22×10^{15} Bq



Gamma-ray source of 4.1×10^{15} Bq

Figure 2.1 Relations between absorbed dose rate and distance from the gamma-ray sources. Activity of the sources is 4.1×10^{15} Bq, and 0.22×10^{15} Bq, respectively. The absorbed dose rate was defined as that for air.

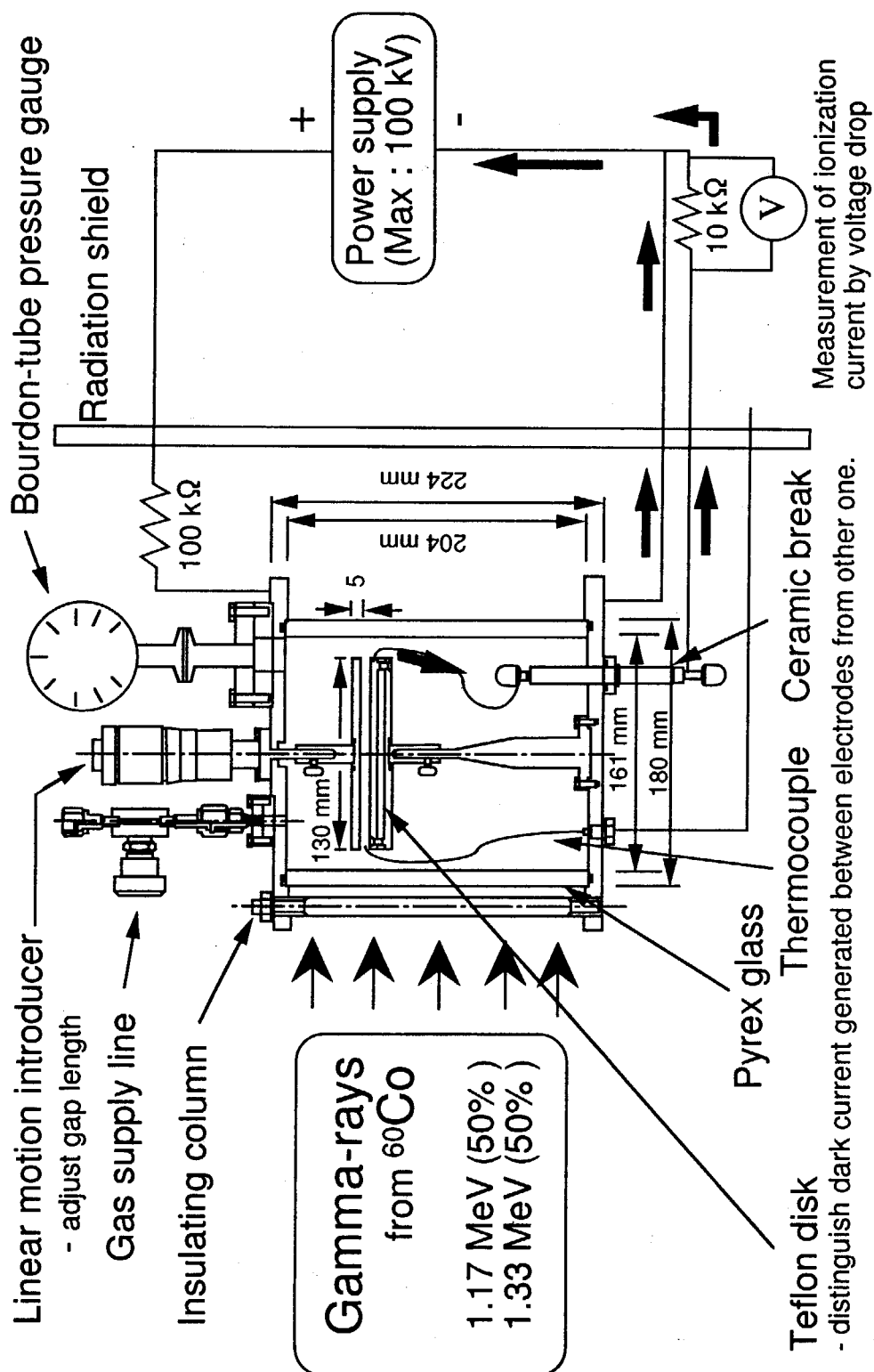


Figure 2.2 Experimental apparatus for measuring ionization current and breakdown voltage. This apparatus is pumped to vacuum and then is filled with test gas through the gas supply line.

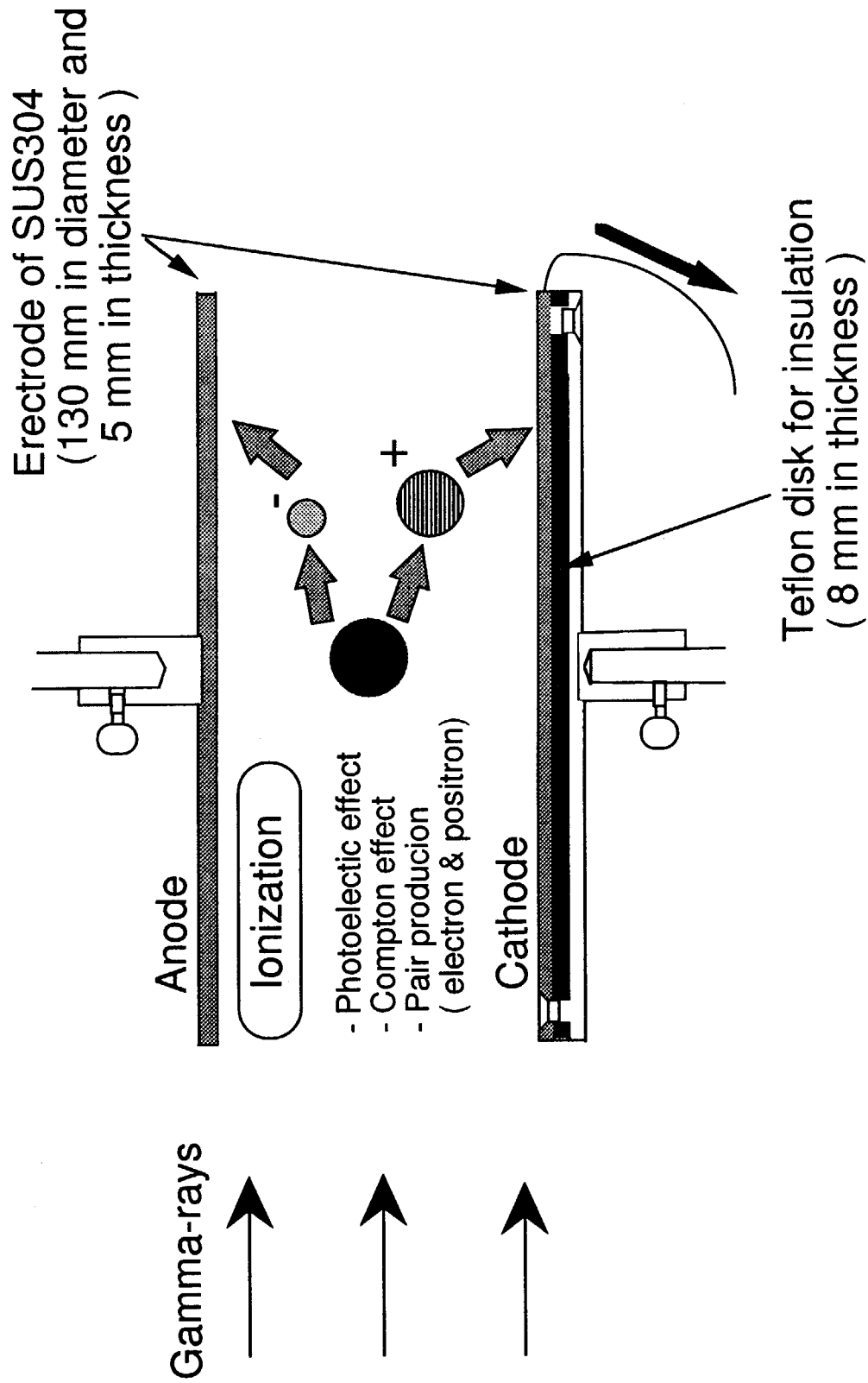


Figure 2.3 Interactions between gamma rays and molecules: ionization current flows when positive particles reach the cathode electrode.

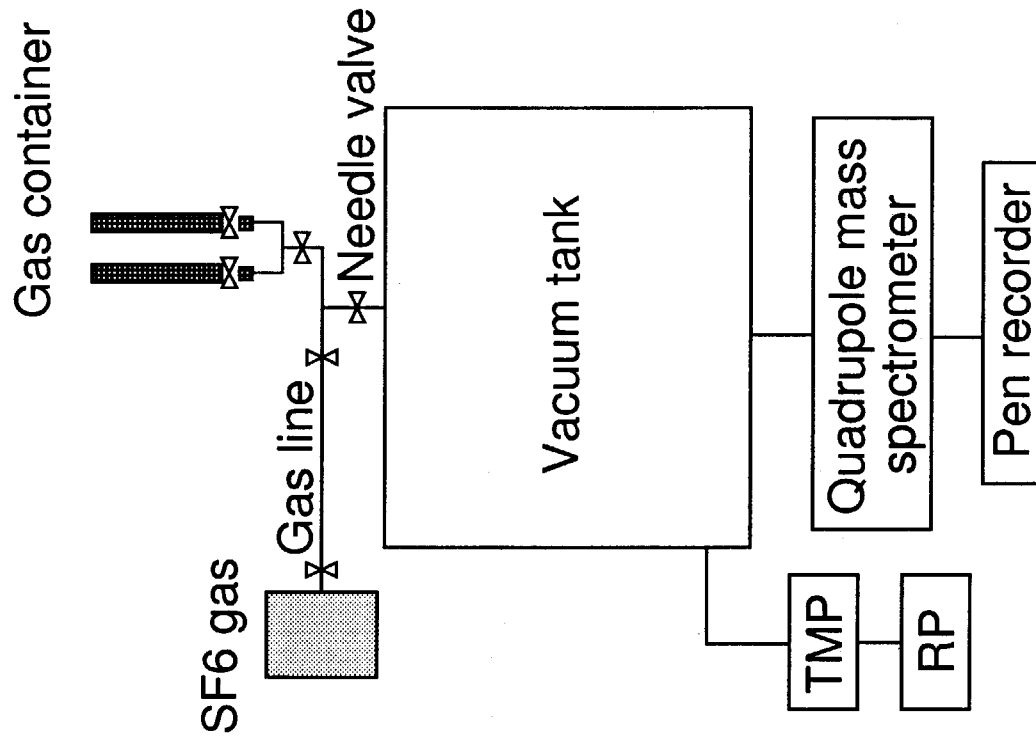


Figure 2.4 Experimental apparatus for analyzing dissociative products of SF_6 gas. The dissociative products were analyzed with a quadrupole mass spectrometer measuring mass spectra up to $m/e=200$.

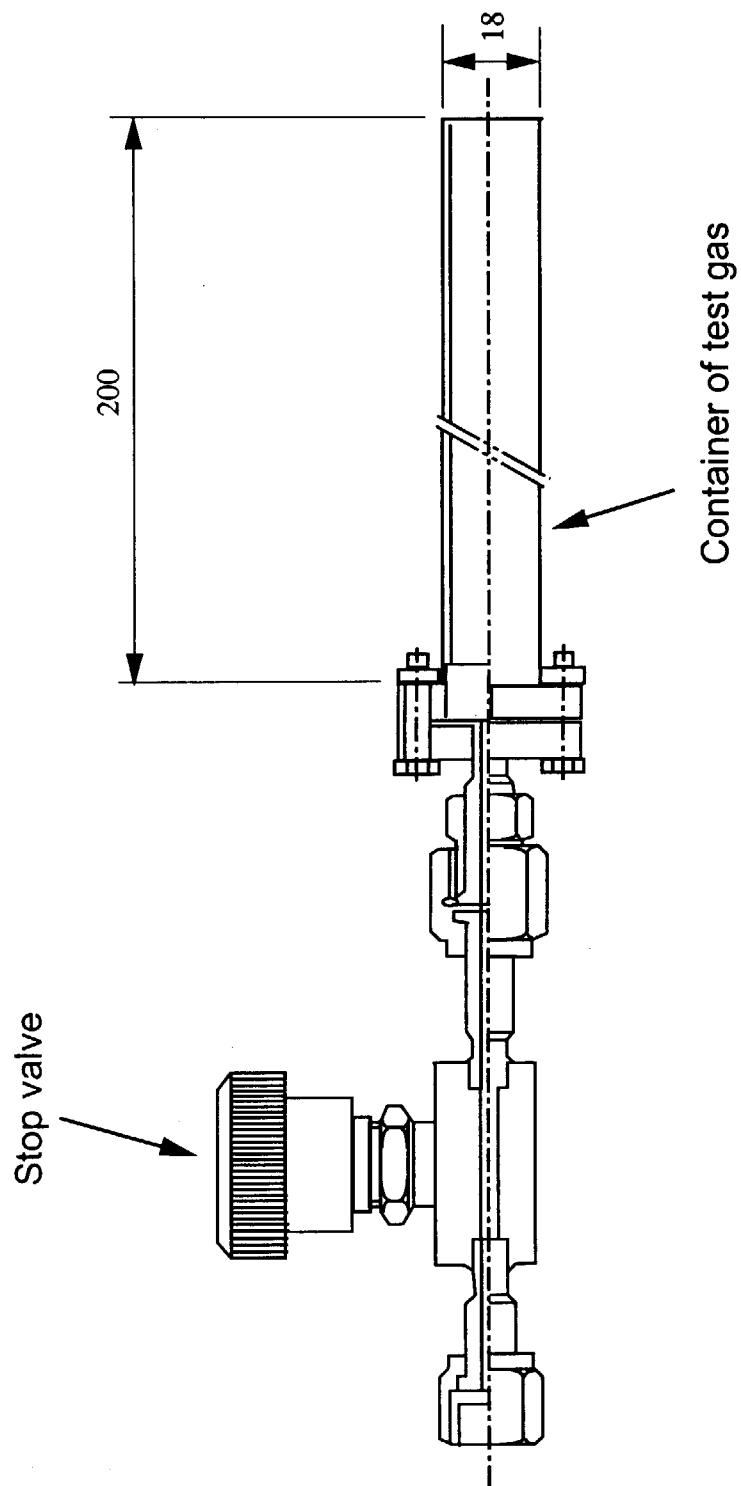


Figure 2.5 Test ampule is filled with SF₆ gas after baked and then cooled down.

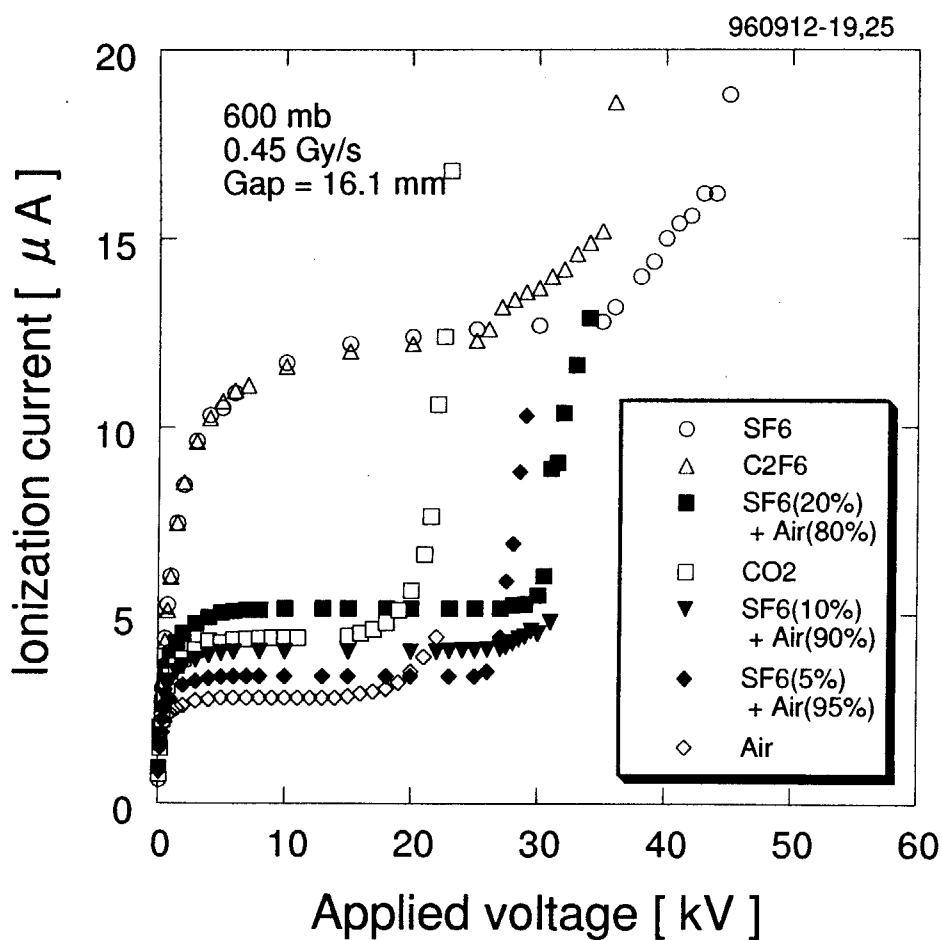


Figure 3.1 Ionization currents of insulating gases against voltage applied between the electrodes. Gas pressure was 600 mb(0.59 MPa), and absorbed dose rate was 0.45 Gy/s.

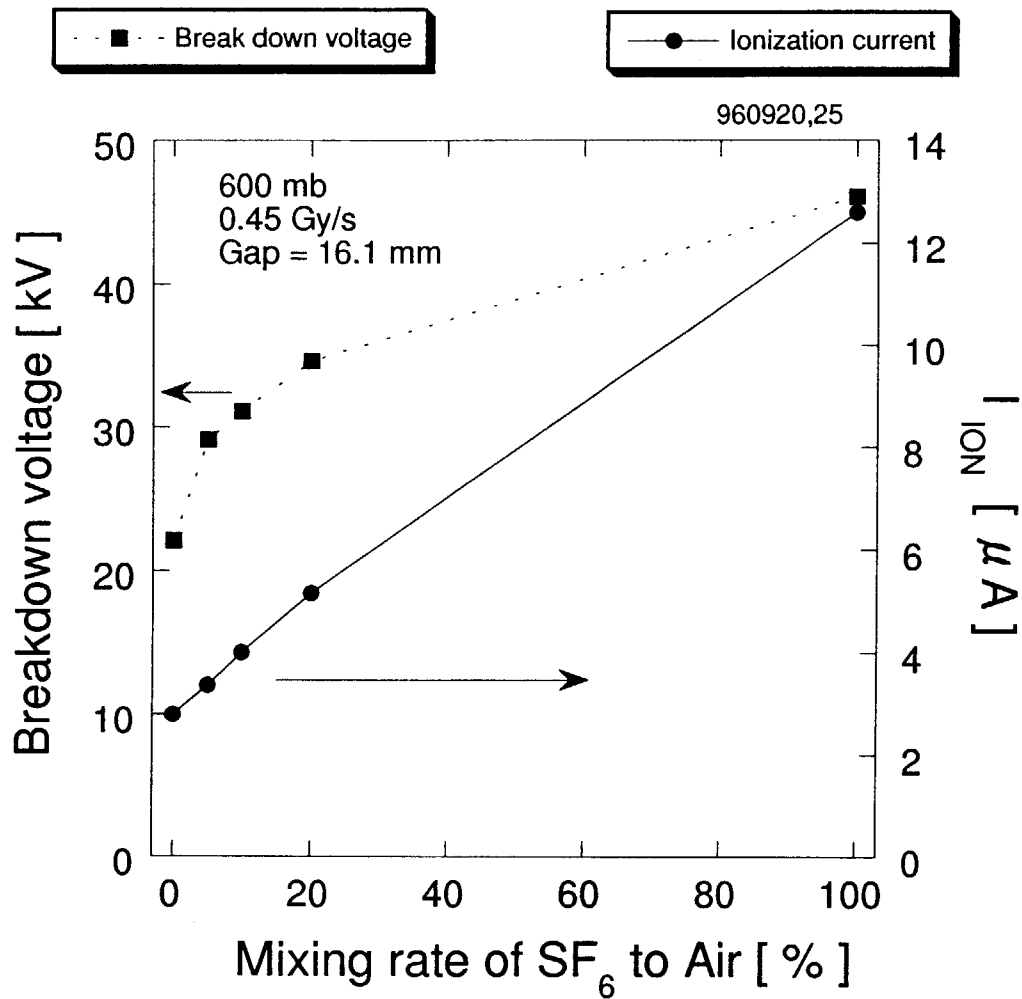


Figure 3.2 Breakdown voltage and ionization current of SF_6 mixed with air. New term of I_{ION} was defined as the ionization current at a half voltage of breakdown voltage.

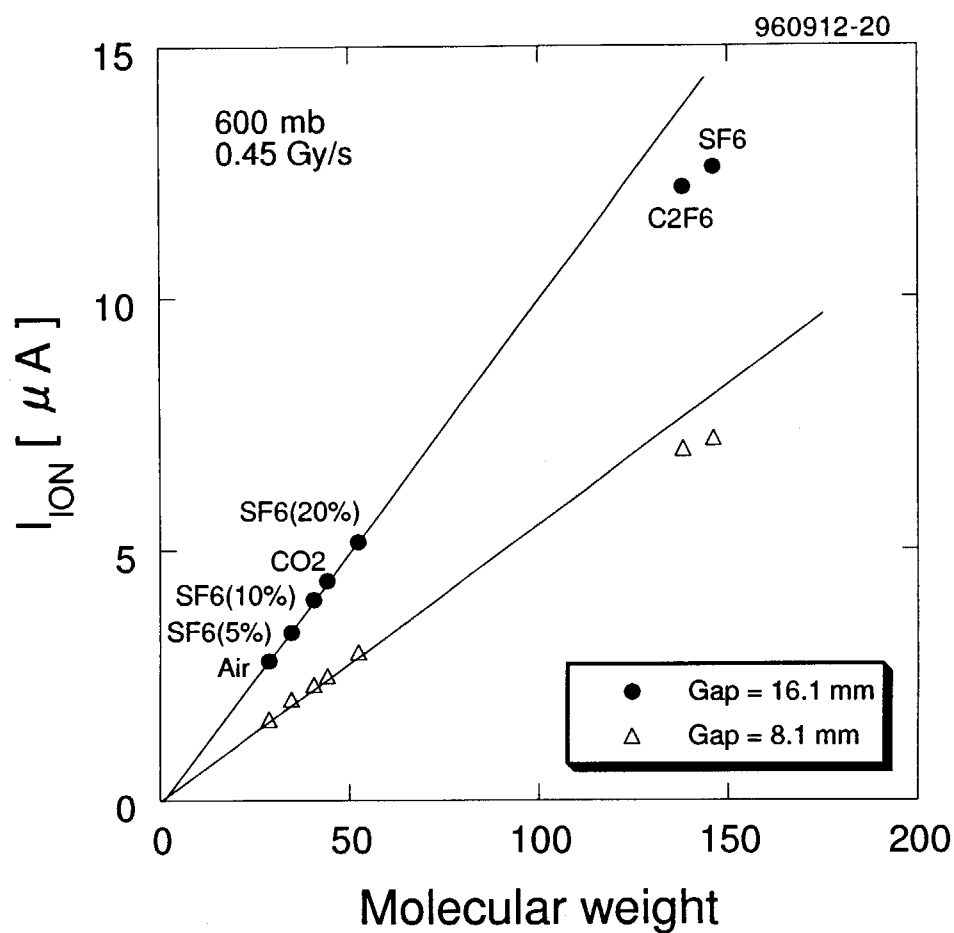


Figure 3.3 I_{ION} as a function of molecular weight. Molecular weight of mixing gases was defined as average one that is sum of molecular weight multiplied by ratio of partial pressure.

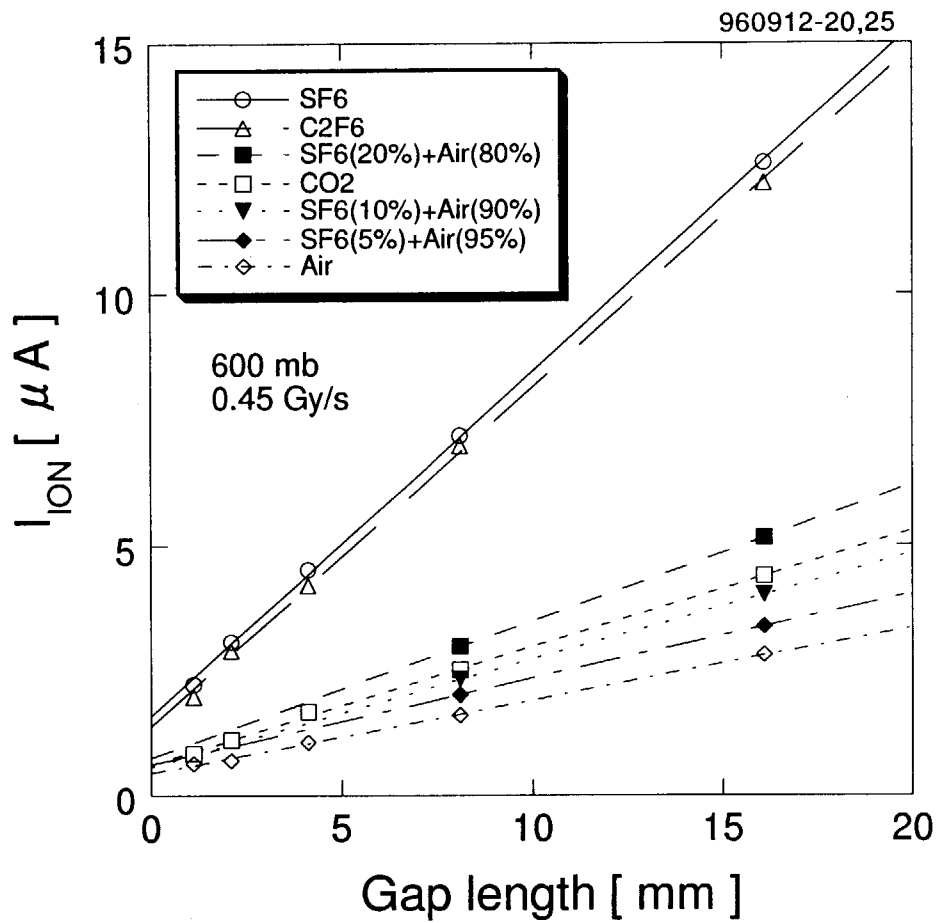


Figure 3.4 I_{ION} as a function of the gap length between the electrodes. Linear relationship between I_{ION} and the gap length indicates that there will be linear relationship between I_{ION} and the volume of gas.

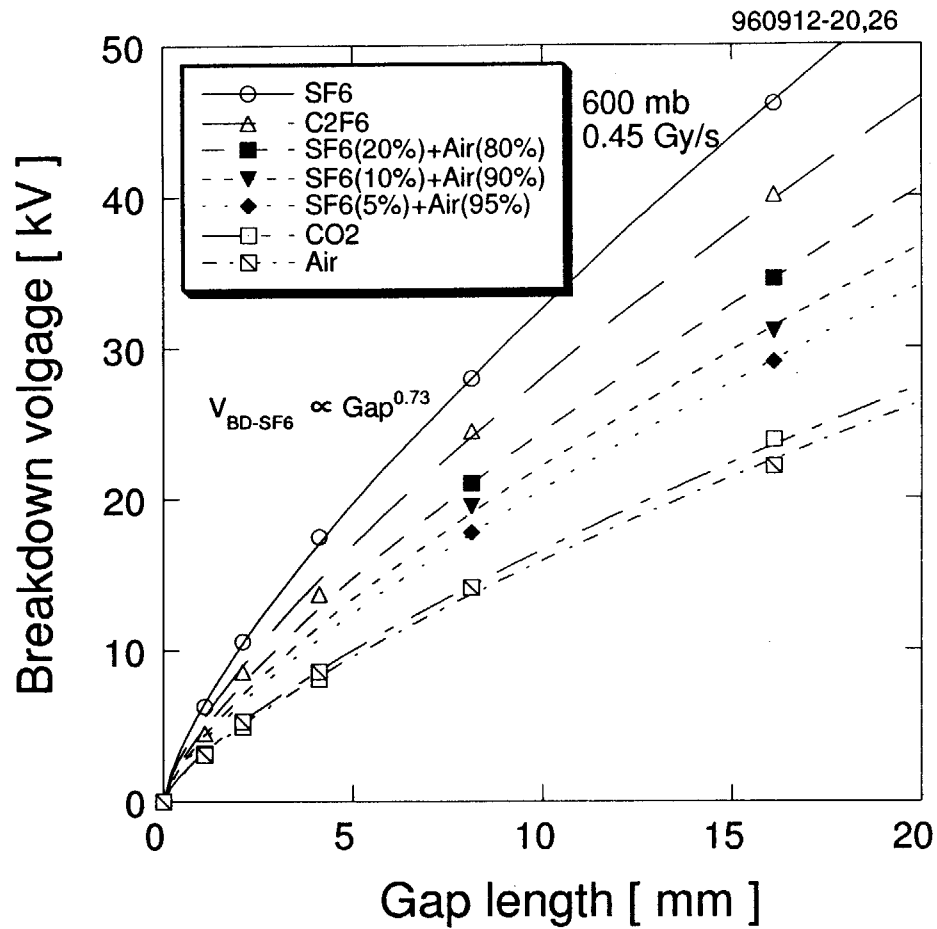


Figure 3.5 Breakdown voltage of gases as a function of the gap length. As for all gases, breakdown voltage increased with the gap length to the 0.73.

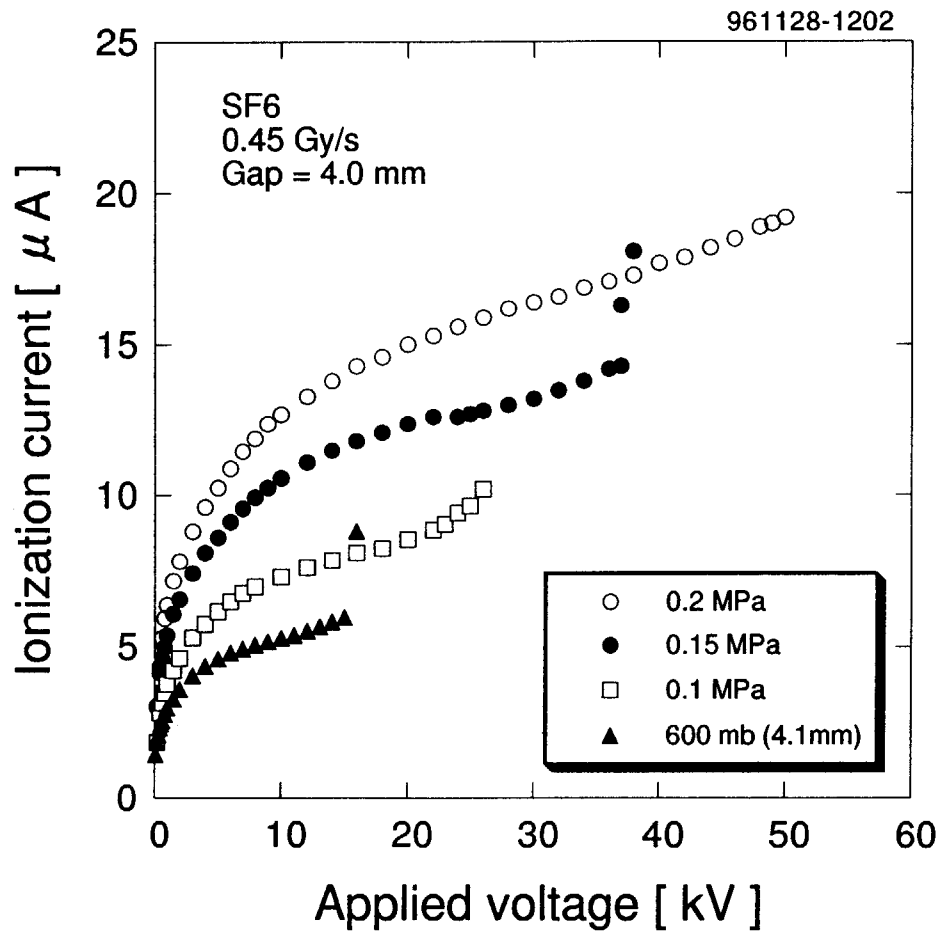


Figure 3.6 Ionization current of SF₆ as a function of applied voltage. The ionization current was measured at several gas pressure.

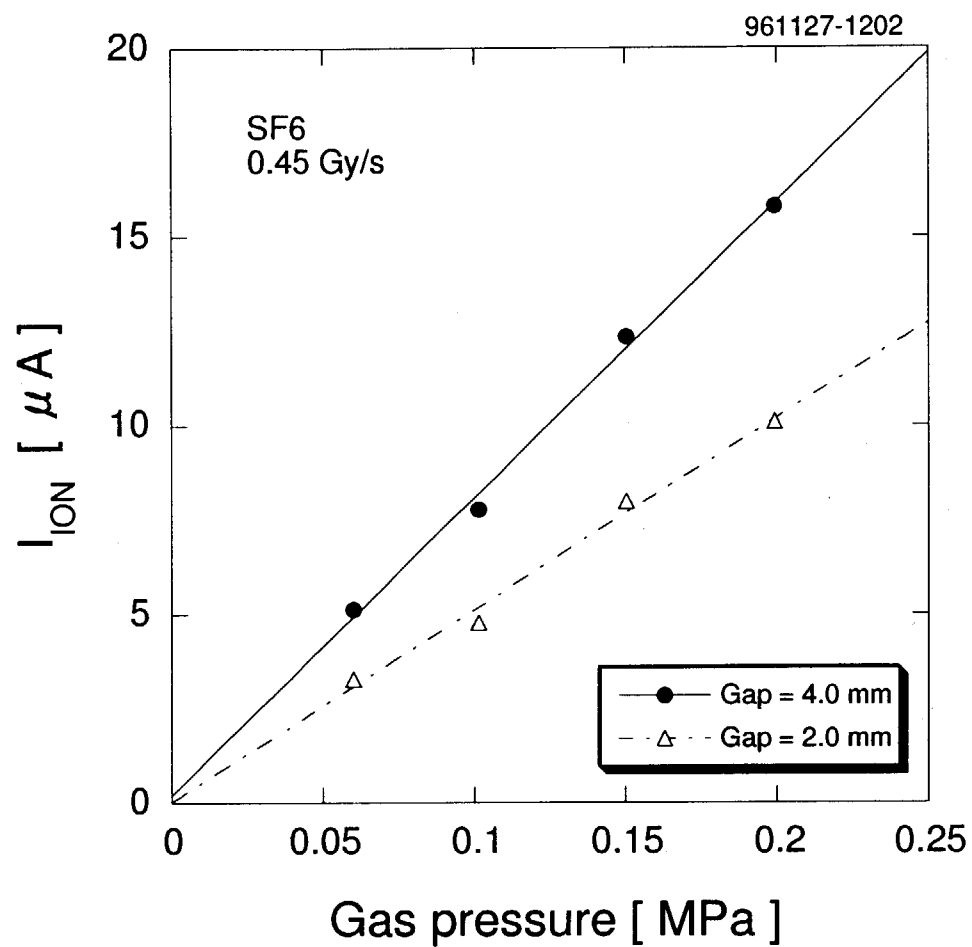


Figure 3.7 I_{ION} as a function of gas pressure. The I_{ION} increased linearly with gas pressure.

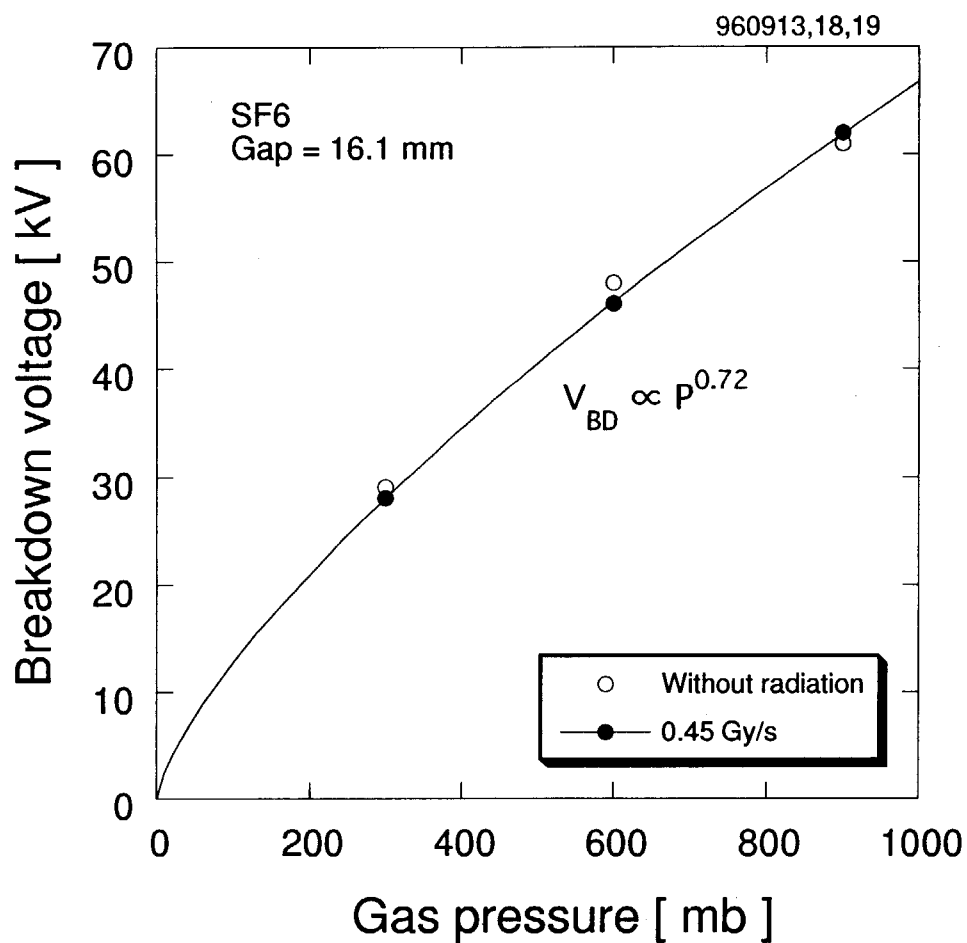


Figure 3.8 Breakdown voltage as a function of gas pressure. At both irradiation and non-irradiation, breakdown voltage increased with gas pressure to the 0.72.

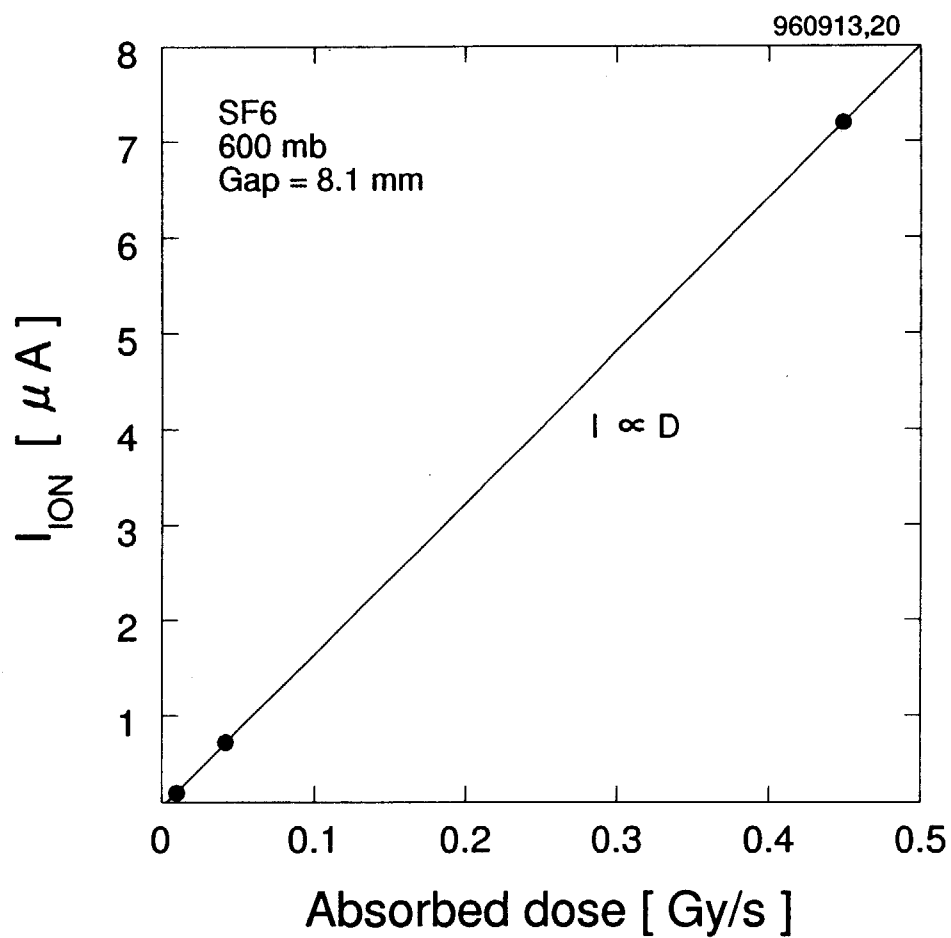


Figure 3.9 I_{ION} as a function of absorbed dose rate. The I_{ION} increased linearly with absorbed dose rate.

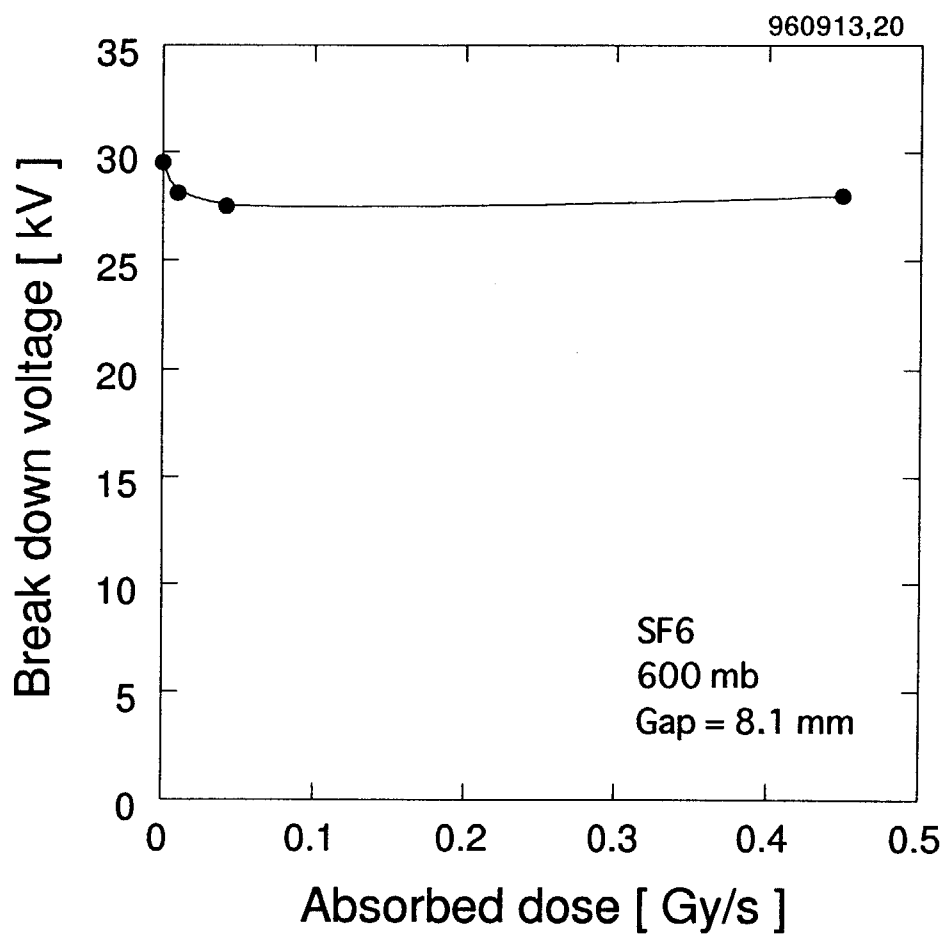
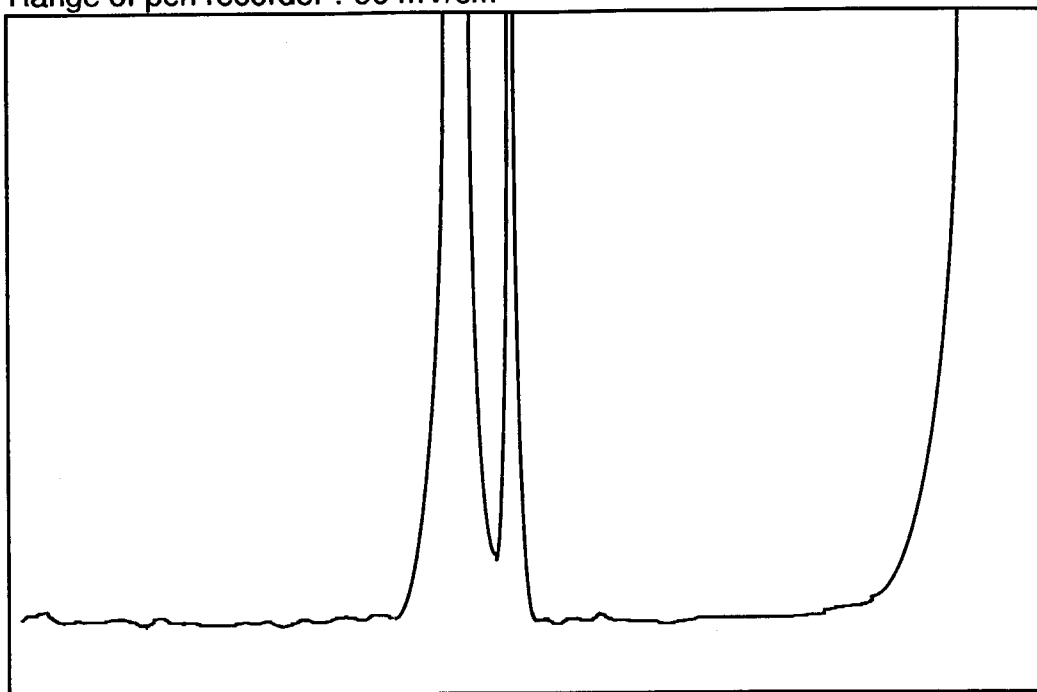


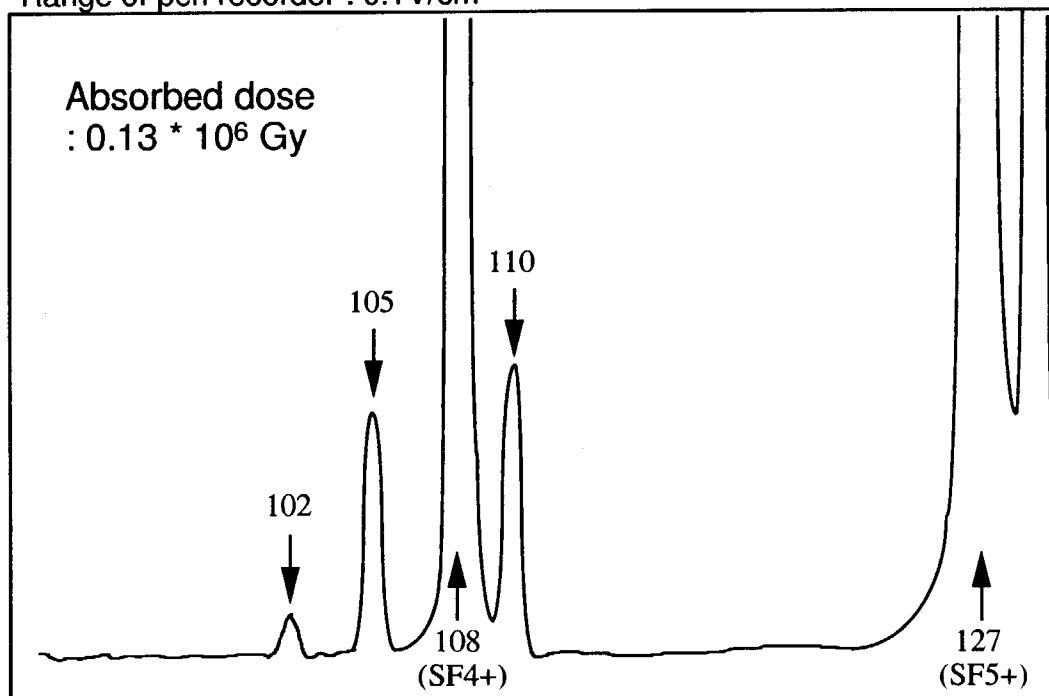
Figure 3.10 Breakdown voltage as a function of absorbed dose rate. The breakdown voltage during irradiation was about 10% lower than that without irradiation.

Range of pen recorder : 50 mV/cm



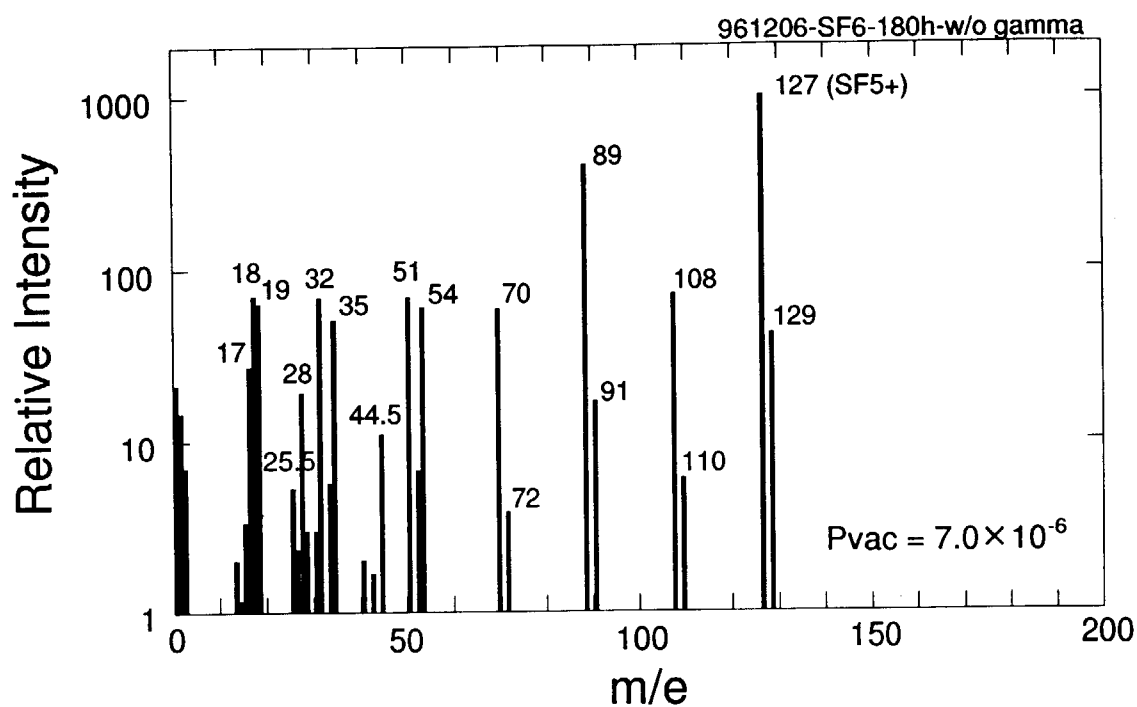
A part of a mass spectrum of SF₆ without irradiation

Range of pen recorder : 0.1 V/cm

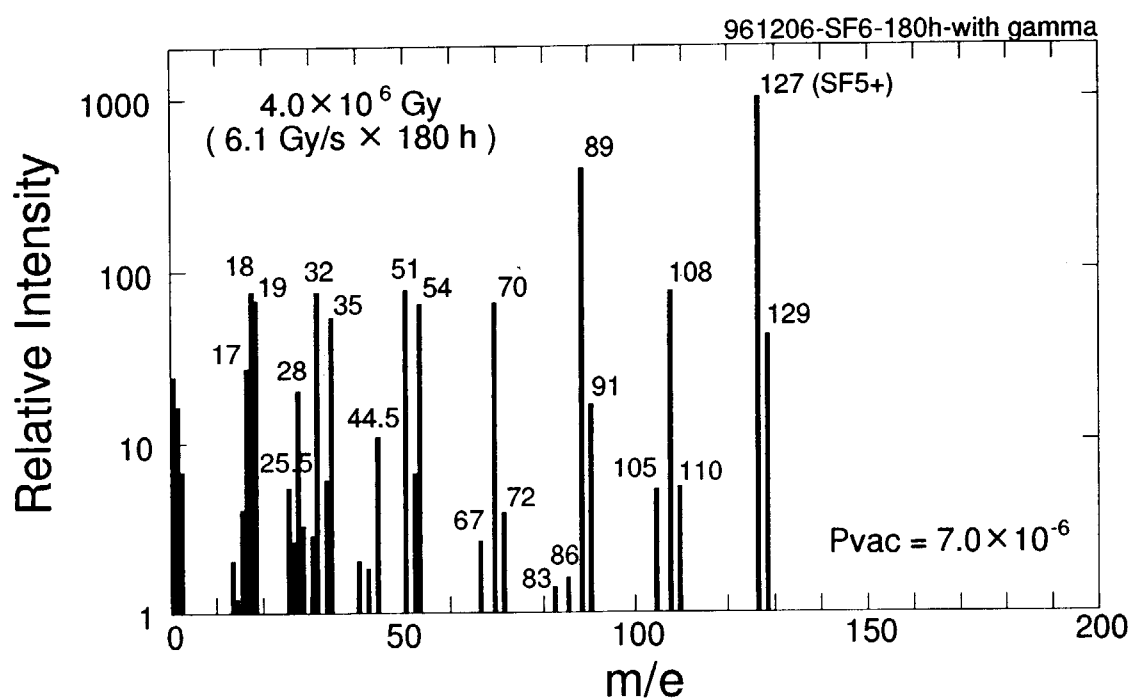


A part of a mass spectrum of SF₆ after irradiation

Figure 3.11 Mass spectra of SF₆ gas. Upper side of the figure is a part of a mass spectrum without irradiation. Lower side is a part of that after irradiation.



A mass spectrum of SF₆ without irradiation



A mass spectrum of SF₆ after irradiation

Figure 3.12 Mass spectra from m/e=0 to 200. Upper side of the figure is a mass spectrum without irradiation. Lower side is that after irradiation of 4.0×10^6 Gy.

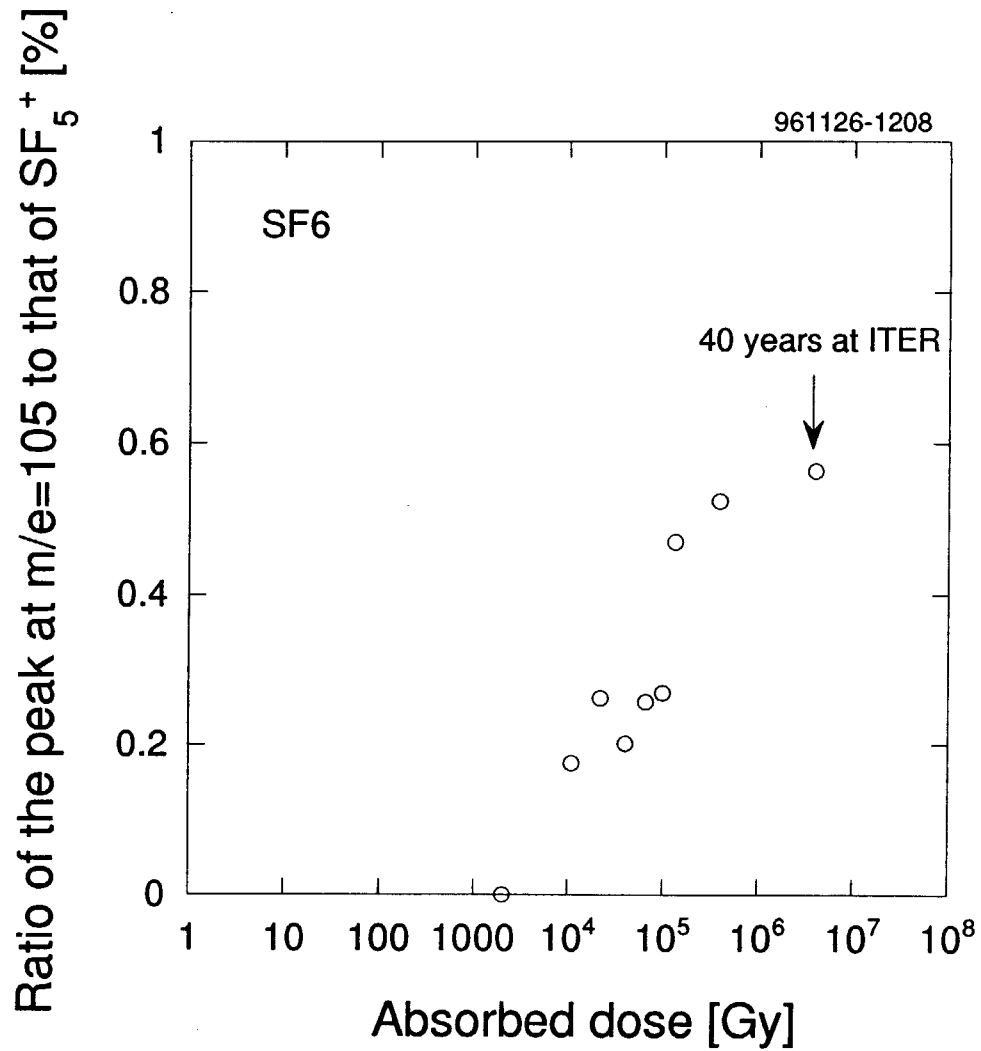


Figure 3.13 Ratio of $m/e=105$ to $m/e=127$ (SF_5^+). The height of each peak was compared. The ratio was saturated with absorbed dose.

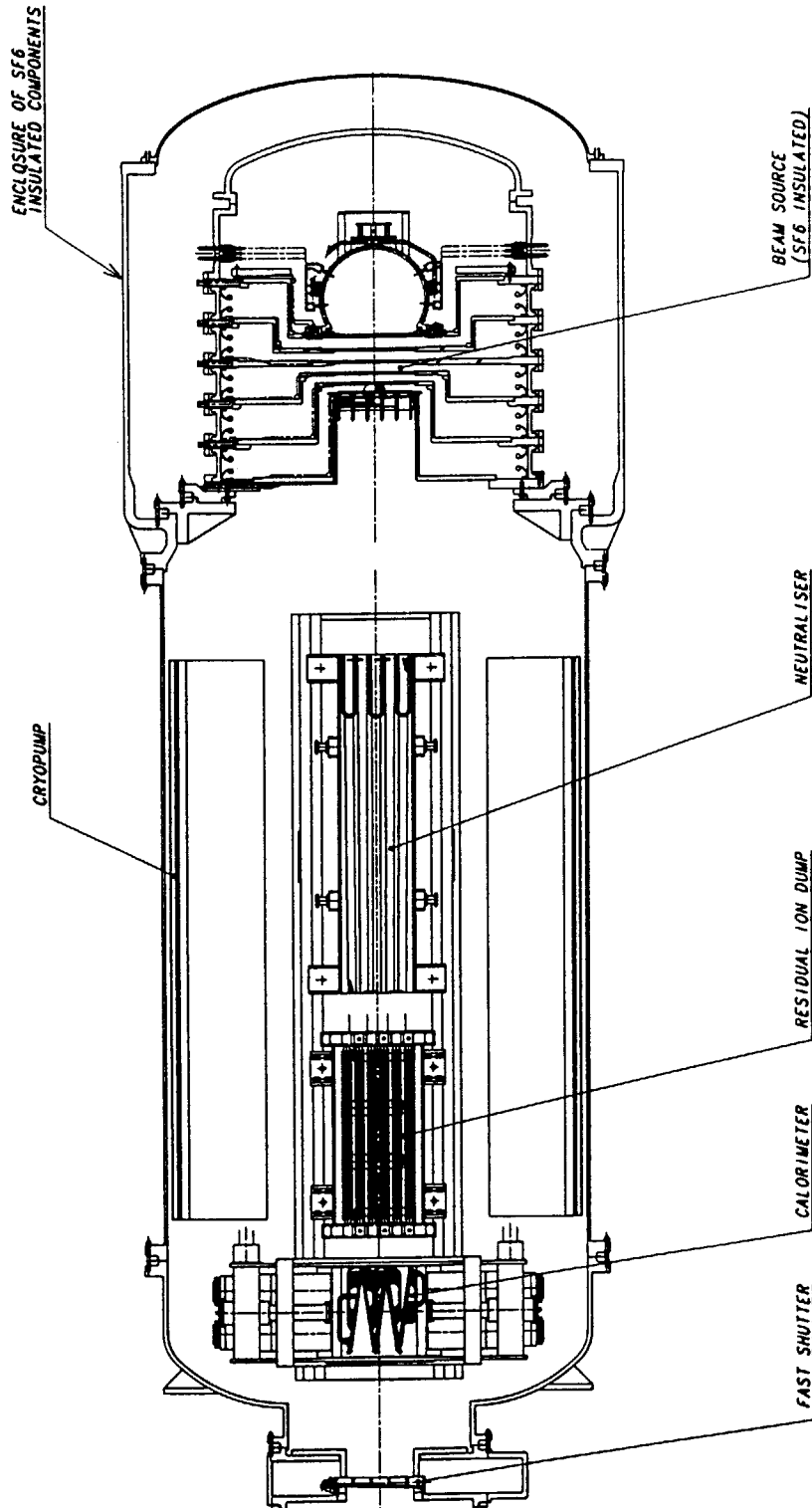


Figure 4.1 Cross section of the ITER-NBI module. The beam source is surrounded with SF₆ gas for insulation.

This is a blank page.

国際単位系 (SI) と換算表

表1 SI基本単位および補助単位

量	名称	記号
長さ	メートル	m
質量	キログラム	kg
時間	秒	s
電流	アンペア	A
熱力学温度	ケルビン	K
物質	モル	mol
光	カンデラ	cd
平面角	ラジアン	rad
立体角	ステラジアン	sr

表3 固有の名称をもつSI組立単位

量	名称	記号	他のSI単位による表現
周波数	ヘルツ	Hz	s^{-1}
力	ニュートン	N	$m \cdot kg / s^2$
圧力, 応力	パスカル	Pa	N / m^2
エネルギー, 仕事, 熱量	ジュール	J	$N \cdot m$
工率, 放射束	ワット	W	J / s
電気量, 電荷	クーロン	C	$A \cdot s$
電位, 電圧, 起電力	ボルト	V	W / A
静電容量	ファラド	F	C / V
電気抵抗	オーム	Ω	V / A
コンダクタンス	ジーメン	S	A / V
磁束	ウェーバ	Wb	$V \cdot s$
磁束密度	テスラ	T	Wb / m^2
インダクタンス	ヘンリー	H	Wb / A
セルシウス温度	セルシウス度	$^{\circ}C$	
光束	ルーメン	lm	$cd \cdot sr$
照度	ルクス	lx	lm / m^2
放射能	ベクレル	Bq	s^{-1}
吸収線量	グレイ	Gy	J / kg
線量等量	シーベルト	Sv	J / kg

表2 SIと併用される単位

名称	記号
分, 時, 日	min, h, d
度, 分, 秒	$^{\circ}, ', ''$
リットル	l, L
トン	t
電子ボルト	eV
原子質量単位	u

$$1 \text{ eV} = 1.60218 \times 10^{-19} \text{ J}$$

$$1 \text{ u} = 1.66054 \times 10^{-27} \text{ kg}$$

表4 SIと共に暫定的に維持される単位

名称	記号
オングストローム	\AA
バーン	b
バル	bar
ガリ	Gal
キュリー	Ci
レントゲン	R
ラド	rad
レム	rem

$$1 \text{ \AA} = 0.1 \text{ nm} = 10^{-10} \text{ m}$$

$$1 \text{ b} = 100 \text{ fm} = 10^{-28} \text{ m}^2$$

$$1 \text{ bar} = 0.1 \text{ MPa} = 10^5 \text{ Pa}$$

$$1 \text{ Gal} = 1 \text{ cm/s}^2 = 10^{-2} \text{ m/s}^2$$

$$1 \text{ Ci} = 3.7 \times 10^{10} \text{ Bq}$$

$$1 \text{ R} = 2.58 \times 10^{-4} \text{ C/kg}$$

$$1 \text{ rad} = 1 \text{ cGy} = 10^{-2} \text{ Gy}$$

$$1 \text{ rem} = 1 \text{ cSv} = 10^{-2} \text{ Sv}$$

表5 SI接頭語

倍数	接頭語	記号
10^{18}	エクサ	E
10^{15}	ペタ	P
10^{12}	テラ	T
10^9	ギガ	G
10^6	メガ	M
10^3	キロ	k
10^2	ヘクト	h
10^1	デカ	da
10^{-1}	デシ	d
10^{-2}	センチ	c
10^{-3}	ミリ	m
10^{-6}	マイクロ	μ
10^{-9}	ナノ	n
10^{-12}	ピコ	p
10^{-15}	フェムト	f
10^{-18}	アト	a

(注)

- 表1～5は「国際単位系」第5版, 国際度量衡局1985年刊行による。ただし, 1 eV および 1 u の値はCODATAの1986年推奨値によった。
- 表4には海里, ノット, アール, ヘクタールも含まれているが日常の単位なのでここでは省略した。
- bar は, JISでは流体の圧力を表わす場合に限り表2のカテゴリーに分類されている。
- E C閣僚理事会指令では bar, barn および「血圧の単位」 mmHg を表2のカテゴリーに入れている。

換算表

力	N (=10 ⁵ dyn)	kgf	lbf
	1	0.101972	0.224809
	9.80665	1	2.20462
	4.44822	0.453592	1

$$\text{粘度} \quad 1 \text{ Pa} \cdot \text{s} (N \cdot \text{s} / m^2) = 10 \text{ P (ポアズ)} (g / (cm \cdot s))$$

$$\text{動粘度} \quad 1 m^2 / s = 10^4 \text{ St (ストークス)} (cm^2 / s)$$

圧	MPa (=10 bar)	kgf/cm ²	atm	mmHg (Torr)	lbf/in ² (psi)
	1	10.1972	9.86923	7.50062×10^3	145.038
力	0.0980665	1	0.967841	735.559	14.2233
	0.101325	1.03323	1	760	14.6959
	1.33322×10^{-4}	1.35951×10^{-3}	1.31579×10^{-3}	1	1.93368×10^{-2}
	6.89476×10^{-3}	7.03070×10^{-2}	6.80460×10^{-2}	51.7149	1

エネルギー・仕事・熱量	J (=10 ⁷ erg)	kgf·m	kW·h	cal (計量法)	Btu	ft·lbf	eV
	1	0.101972	2.77778×10^{-7}	0.238889	9.47813×10^{-4}	0.737562	6.24150×10^{18}
	9.80665	1	2.72407×10^{-6}	2.34270	9.29487×10^{-3}	7.23301	6.12082×10^{19}
	3.6×10^5	3.67098×10^5	1	8.59999×10^5	3412.13	2.65522×10^6	2.24694×10^{25}
	4.18605	0.426858	1.16279×10^{-6}	1	3.96759×10^{-3}	3.08747	2.61272×10^{19}
	1055.06	107.586	2.93072×10^{-4}	252.042	1	778.172	6.58515×10^{21}
	1.35582	0.138255	3.76616×10^{-7}	0.323890	1.28506×10^{-3}	1	8.46233×10^{18}
	1.60218×10^{19}	1.63377×10^{20}	4.45050×10^{-26}	3.82743×10^{-20}	1.51857×10^{-22}	1.18171×10^{19}	1

$$1 \text{ cal} = 4.18605 \text{ J (計量法)}$$

$$= 4.184 \text{ J (熱化学)}$$

$$= 4.1855 \text{ J (15}^{\circ}\text{C)}$$

$$= 4.1868 \text{ J (国際蒸気表)}$$

$$\text{仕事率} \quad 1 \text{ PS (仏馬力)}$$

$$= 75 \text{ kgf} \cdot \text{m/s}$$

$$= 735.499 \text{ W}$$

放射能	Bq	Ci
	1	2.70270×10^{-11}
	3.7×10^{10}	1

吸収線量	Gy	rad
	1	100
	0.01	1

照射線量	C/kg	R
	1	3876
	2.58×10^{-4}	1

線量当量	Sv	rem
	1	100
	0.01	1

EXPERIMENTAL STUDY ON THE INFLUENCE OF RADIATION ON HIGH-VOLTAGE INSULATION GASES